



Department of Mathematics and Computer Science

Convergence of Adaptive Finite Element Methods for the Poisson Problem

Master Thesis

Submitted by: Ines Perko

Supervisor: Univ.-Prof. Dr. Volker John
Second Reviewer: Dr. Alfonso Caiazzo

Berlin, July 30, 2020

Selbstständigkeitserklärung

Name: PERKO	(Nur Block- oder Maschinenschrift verwenden.)
Vorname: INES	
geb.am: 22.11.1993	
Matr.Nr.: 5197234	

Ich erkläre gegenüber der Freien Universität Berlin, dass ich die vorliegende MASTERARBEIT selbstständig und ohne Benutzung anderer als der angegebenen Quellen und Hilfsmittel angefertigt habe.

Die vorliegende Arbeit ist frei von Plagiaten. Alle Ausführungen, die wörtlich oder inhaltlich aus anderen Schriften entnommen sind, habe ich als solche kenntlich gemacht.

Diese Arbeit wurde in gleicher oder ähnlicher Form noch bei keiner anderen Universität als Prüfungsleistung eingereicht.

Datum: 30.07.2020

Unterschrift: Ines Perko

Contents

1	Introduction	1
2	Finite Element Methods	3
2.1	Lebesgue spaces and Sobolev spaces	3
2.2	Model problem	8
2.3	Conforming Finite Element discretization	10
2.4	A priori estimate of the error in the L^2 norm of gradient	12
2.5	Neumann and Dirichlet cases	16
3	A Posteriori Error Estimators	20
3.1	Goals	20
3.2	Adaptive algorithm	21
3.3	Residual a posteriori error estimates	21
3.4	Ways for refining the mesh	25
4	Convergence of an adaptive algorithm	30
5	Numerical Studies	34
6	Conclusion and Outlook	44
6.1	Conclusion	44
6.2	Outlook	44
	List of figures	46
	List of tables	46
	References	47
	Appendix A Tools from the Analysis	50
	Nomenclature	58

1 Introduction

Many physical problems arising in engineering and science can be mathematically modeled and expressed through partial differential equations. Since analytical solutions of these equations cannot be explicitly computed in general, numerical methods for finding approximate solutions, such as the finite element methods are used. With its roots in the 1940s [Cou43], and further development through the 1950s to 1970s by engineers and mathematicians, the first book that focused on the mathematical foundations is [SF73], published in 1973. Nowadays, many physical and chemical phenomena apply finite element methods to solve them since this method easily handles boundary conditions, complex geometry and because of its clear structure it is possible to develop a software for applications. From the mathematical side, the function spaces are needed for the presentation of the finite element method. More precisely, the Lebesgue and Sobolev spaces presented in this thesis are sufficient. Furthermore, the variational formulation of the partial differential equation should be obtained. Here, the model problem is the Poisson equation with Dirichlet-Neumann boundary conditions, on which the finite element method will be developed. The model problem is rewritten in its variational formulation and the existence and uniqueness of the solution are proven. Knowing that the solution exists, an approximation is done by finite elements. In the late 1970s, the concept of adaptivity was developed within the framework of finite element methods. The method is called the adaptive finite element method. Its importance and potential come from its concept where automatic adjustment is done to improve approximations. The adaptive method handles practical problems in solid and fluid mechanics, in porous media flow and semiconductor device simulation [BS08] and provides the optimal overall accuracy of the numerical approximations, since in these cases local singularities might be present and therefore the overall accuracy decreases. One of the first works that presented the idea of this method based on the error estimates is [BR78]. In particular, the a posteriori error estimators are shown as a necessity for adaptivity. They are important for the evaluation of the reliability of the results as well as controlling the refinement process, which is a crucial process in this method.

The main goal of the thesis is to show the convergence of adaptive finite element methods for the Poisson problem. The proof presented here follows [Ver13], and it is based on the Poisson problem with pure Dirichlet boundary conditions. The adaptive method is presented through the adaptive algorithm [Ver13, Algorithm 1.1]. To make this algorithm effective, an error indicator which supplies the a posteriori error estimate should be chosen along with a reliable refinement strategy. In the proof here, for the a posteriori error estimates, the residual estimates are utilized. They estimate the error of the numerical solution by a norm of its residual. Specifically, for this algorithm, the error estimator in the L^2 -norm of the gradient is used. The first proof of the convergence based on a posteriori error estimates was published in [D96] in 1996. Nowadays, these results are improved and a lot of literature is based on the idea presented in [D96]. Some of the improvements are simultaneous control of the error indicator and the data oscillation [MNS02].

Chapter 2 provides the mathematical theory required for the development of the finite element method. Also, the a priori estimate of the error in the L^2 -norm of gradient is introduced. The chapter ends with an inspection of the

different values for Dirichlet and Neumann boundary conditions.

Chapter 3 presents the adaptive algorithm along with all the necessary data for it. Therefore, the residual a posteriori error estimates that provide upper and lower bounds for the error are introduced as well as the residual a posteriori error indicator. The marking strategies are presented and the processes of refinement, coarsening, and smoothing of meshes that obtain the adaptive discretizations are described.

After having successfully defined data and making an adaptive algorithm effective, chapter 4 proves the convergence of it. The idea is to show that by every iteration of the algorithm, the error is reduced at least by some factor.

Chapter 5 describes the numerical results of the simulations of the two examples which consider the Poisson equation. The properties of the interest are discussed and the obtained results support the convergence of the adaptive algorithm. Chapter 6 presents the conclusion and the outlook of the thesis.

2 Finite Element Methods

2.1 Lebesgue spaces and Sobolev spaces

This chapter starts with definitions and basic properties of the Lebesgue spaces and Sobolev spaces following the literature [AF03], [OR76], [Maz85], [BS08], [Che05], [Gri11], [DD12], and [Ada75].

Let the domain Ω be an open, non-empty set in n -dimensional real Euclidean space \mathbb{R}^n . The standard Lebesgue spaces are denoted with $L^p(\Omega)$, whenever $1 \leq p < \infty$. The space $L^p(\Omega)$ is the space of Lebesgue measurable functions u defined on Ω for which

$$\int_{\Omega} |u(x)|^p dx < \infty. \quad (1)$$

The norm on $L^p(\Omega)$, which is denoted by $\|\cdot\|_{L^p(\Omega)}$, is defined by

$$\|u\|_{L^p(\Omega)} = \left(\int_{\Omega} |u(x)|^p dx \right)^{\frac{1}{p}}. \quad (2)$$

Positivity and homogeneity follow from the definition and the inequality that is used for the triangle inequality is

$$\|u + v\|_{L^p(\Omega)} \leq \|u\|_{L^p(\Omega)} + \|v\|_{L^p(\Omega)}.$$

This inequality is also known as Minkowski's inequality. Therefore, this is a normed space. In $L^p(\Omega)$ one identifies functions which are equal almost everywhere in Ω . Thus, the elements of Lebesgue spaces are equivalence classes of the functions u defined on Ω satisfying (1). For the case $p = \infty$, one gets the space of essentially bounded Lebesgue measurable functions. This Lebesgue's space is denoted by $L^\infty(\Omega)$. As a norm, one can take its essential supremum, i.e.,

$$\|u\|_{L^\infty(\Omega)} = \text{ess sup}_{x \in \Omega} |u(x)|. \quad (3)$$

Another fundamental inequality in $L^p(\Omega)$ spaces is Hölder's inequality.

Theorem 2.1. (Hölder's inequality) *Let $1 \leq p, q \leq \infty$ such that $\frac{1}{p} + \frac{1}{q} = 1$. If $u \in L^p(\Omega)$ and $v \in L^q(\Omega)$, then $uv \in L^1(\Omega)$ and*

$$\int_{\Omega} |u(x)v(x)| dx \leq \|u\|_{L^p(\Omega)} \|v\|_{L^q(\Omega)}. \quad (4)$$

Proof. The proof can be found in [AF03], Theorem 2.16. \square

One of the basic properties of the Lebesgue spaces $L^p(\Omega)$ is that they are Banach spaces for $1 \leq p \leq \infty$. For the case $p = 2$, one gets the space $L^2(\Omega)$. That is a Hilbert space with respect to the inner product

$$(u, v) = \int_{\Omega} u(x) \overline{v(x)} dx. \quad (5)$$

Hölder's inequality in $L^2(\Omega)$ space is called Cauchy's or Schwarz's inequality.

Furthermore, the space $C_0^\infty(\Omega)$ of test functions on Ω should be introduced. It is the subset of the space $C^\infty(\Omega)$ which consists of the functions from $C^\infty(\Omega)$ on Ω with compact support in Ω , i.e.,

$$C_0^\infty(\Omega) = \{\varphi \in C^\infty(\Omega) \mid \text{supp}\varphi \text{ is compact in } \Omega\}. \quad (6)$$

In other words, a test function is a function that has continuous derivatives of all orders but it will vanish outside of some bounded set thanks to the compact support. Thus, when Ω is bounded, it is equivalent to saying that u vanishes in a neighborhood of the boundary Γ of Ω . The space $C_0^\infty(\Omega)$ is contained in the most of the spaces defined in connection with Ω as $C_0^\infty(\Omega) \subset L^p(\Omega)$, for $1 \leq p \leq \infty$.

Corollary 2.1. $C_0^\infty(\Omega)$ is dense in $L^p(\Omega)$ if $1 \leq p < \infty$.

Proof. The proof can be found in [AF03], Corollary 2.30. \square

To define the Sobolev spaces, the weak derivative has to be introduced. For that, the following function space is needed.

A function u is locally integrable function if the Lebesgue integral

$$\int_K |u| dx < \infty$$

exists for every compact set $K \subset \Omega$. The space of all locally integrable functions is denoted by $L^1_{loc}(\Omega)$. The space $L^p(\Omega)$ is a subset of the space $L^1_{loc}(\Omega)$ for $1 \leq p \leq \infty$ and any domain Ω .

Let u and w^α be locally integrable on Ω . A function u has a weak derivative w^α of order α if w^α fulfills

$$\int_\Omega w^\alpha \phi dx = (-1)^{|\alpha|} \int_\Omega u D^\alpha \phi dx \quad (7)$$

for every test function $\phi \in C_0^\infty(\Omega)$. Here, w^α is the α th generalized derivative of the u . Whenever the classical derivative $D^\alpha u(x)$ exists, it is also a weak derivative of u . Also, w^α is unique up to a set of measure zero. The concept of the weak derivatives is brought where the classical differentiability fails. Thus, if classical derivatives do not exist, D^α will refer to the weak derivatives.

Sobolev spaces are vector subspaces of different Lebesgue spaces $L^p(\Omega)$. The standard Sobolev space is denoted by $W^{m,p}(\Omega)$, where m is any positive integer and $1 \leq p \leq \infty$. It contains all functions $u \in L^p(\Omega)$ which have all weak derivatives up to order m in $L^p(\Omega)$:

$$W^{m,p}(\Omega) = \{u : D^\alpha u \in L^p(\Omega); \forall \alpha \text{ such that } |\alpha| \leq m\}. \quad (8)$$

The Sobolev norm on the space $W^{m,p}(\Omega)$, for the case $1 \leq p < \infty$ is

$$\|u\|_{W^{m,p}(\Omega)} = \left(\sum_{|\alpha| \leq m} \|D^\alpha u\|_{L^p(\Omega)}^p \right)^{\frac{1}{p}}. \quad (9)$$

For the case $p = \infty$, it is defined as

$$\|u\|_{W^{m,\infty}(\Omega)} = \max_{|\alpha| \leq m} \|D^\alpha u\|_{L^\infty(\Omega)}. \quad (10)$$

One can see that (9) or (10) defines a norm on any vector space of functions on which the right-hand side takes finite values. Therefore, $W^{m,p}(\Omega)$ is a normed space. The following theorem shows that it is complete. Also, one can notice that $W^{0,p}(\Omega)$ is equal to $L^p(\Omega)$.

Theorem 2.2. *$W^{m,p}(\Omega)$ is a Banach space.*

Proof. This proof can be found in [AF03], Theorem 3.3. □

The subspace $C^\infty(\Omega) \cap W^{m,p}(\Omega)$ is dense in $W^{m,p}(\Omega)$. The stronger density condition is that $C_0^\infty(\bar{\Omega})$ is dense in $W^{m,p}(\Omega)$. Whenever the part of the domain lies on both sides of part of its boundary (as occurs with a slit domain) this does not hold. Thus, some regularity conditions must hold to obtain this. The segment condition should be satisfied, i.e., if for every $x \in \Gamma$ there is a neighborhood U_x and a nonzero vector n_x such that if $z \in \bar{\Omega} \cap U_x$ then $z + tn_x \in \Omega$ for $0 < t < 1$. The vector n_x is an inward directed normal to Γ at x . The boundary Γ satisfying this condition must be $(n-1)$ -dimensional. With this density condition, one can always approximate an element of $W^{m,p}(\Omega)$ by smooth bounded functions having bounded derivatives of all orders on Ω .

Furthermore, $W_0^{m,p}(\Omega)$ is a Sobolev space defined as the completion of $C_0^\infty(\Omega)$ with respect to the norm $\|\cdot\|_{W^{m,p}(\Omega)}$. This space can be defined in another way, but first, one should mention imbeddings of the space $W^{m,p}(\Omega)$ into Banach spaces. The most important of the imbedding properties of the spaces $W^{m,p}(\Omega)$ are gathered together under the theorem called the Sobolev Imbedding Theorem, even though they are of different types and they can require different properties and different methods of the proof. One can find more information about it in the [AF03, Chapter IV].

The question which appears is what does imbedding mean for the elements of Sobolev spaces. Elements of $W^{m,p}(\Omega)$ are equivalence classes of functions defined everywhere on Ω equal up to sets of measure zero. To start with, one can look at imbeddings into the continuous function spaces, i.e., $C^j(\bar{\Omega})$, $C_B^j(\Omega)$ and $C^{j,\lambda}(\bar{\Omega})$. For example, observe the existence of imbedding $W^{m,p}(\Omega) \rightarrow C^j(\bar{\Omega})$. That means that each $u \in W^{m,p}(\Omega)$ (when considered as a function) can be redefined on a subset of Ω , which has a zero measure. The new, modified function $v \in C^j(\bar{\Omega})$ is produced in such a way that $v = u$ in $W^{m,p}(\Omega)$ and it satisfies

$$\|v\|_{C^j(\bar{\Omega})} \leq K \|u\|_{W^{m,p}(\Omega)},$$

with K independent of u .

Also, imbeddings can be interpreted as an inclusion relation. Therefore, it provides the ordering among them. For nonnegative integers m and k satisfying $k \leq m$ it holds that

$$W^{m,p}(\Omega) \subset W^{k,p}(\Omega), \quad 1 \leq p \leq \infty. \quad (11)$$

When Ω is bounded it holds that

$$W^{m,p'}(\Omega) \subset W^{m,p}(\Omega), \quad 1 \leq p \leq p' \leq \infty. \quad (12)$$

There exists an operator E called an (m,p) -extension operator for Ω . It maps $W^{m,p}(\Omega)$ into $W^{m,p}(\mathbb{R}^n)$ where Ω has a Lipschitz boundary Γ . As usual, m is a

non negative integer and p is a real number in the range $1 \leq p \leq \infty$. Extension mapping satisfies $Ev|_{\Omega} = v$ for all $u \in W^{m,p}(\Omega)$ and

$$\|Eu\|_{W^{m,p}(\mathbb{R}^n)} \leq C\|u\|_{W^{m,p}(\Omega)}, \quad (13)$$

where C is independent of u .

This property does not hold when Ω does not have Lipschitz boundary. Thus, with the definition of Lipschitz boundary one can now relate Sobolev spaces defined on Ω to those on \mathbb{R}^n . The complementary result is also possible, for any domain where the restriction permits to see functions in $W^{m,p}(\mathbb{R}^n)$ as well defined in $W^{m,p}(\Omega)$. The Sobolev Imbedding Theorem claims the existence of imbeddings of $W^{m,p}(\Omega)$ in $L^q(\Omega)$. If it is proven for \mathbb{R}^n and if domain satisfies stronger regularity conditions, then it must hold for domain Ω as well. Thus, if $W^{m,p}(\mathbb{R}^n) \rightarrow L^q(\mathbb{R}^n)$ and $u \in W^{m,p}(\Omega)$ one can extend the inequality (13) and get the imbedding $W^{m,p}(\Omega) \rightarrow L^q(\Omega)$ through the chain of inequalities:

$$\|u\|_{L^q(\Omega)} \leq \|Eu\|_{L^q(\mathbb{R}^n)} \leq C_2\|Eu\|_{W^{m,p}(\mathbb{R}^n)} \leq C_2C_1\|u\|_{W^{m,p}(\Omega)}.$$

Another inequality that should be introduced is Sobolev's inequality. It presents the relationship between Sobolev spaces with different indices. This inequality also tells that any function with suitable weak derivatives can be interpreted as a continuous and bounded function.

Theorem 2.3. (Sobolev's inequality) *Let $\Omega \subset \mathbb{R}^n$ be a domain with Lipschitz boundary Γ , let m be a positive integer and let p be a real number in the range $1 \leq p < \infty$ such that*

$$\begin{aligned} m &\geq n \text{ when } p = 1, \\ m &> \frac{n}{p} \text{ when } p > 1. \end{aligned}$$

Then there is a constant C such that for all $u \in W^{m,p}(\Omega)$

$$\|u\|_{L^\infty(\Omega)} \leq C\|u\|_{W^{m,p}(\Omega)}.$$

There is a continuous function in the $L^\infty(\Omega)$ equivalence class of u .

Proof. This proof can be found in [BS08], Theorem 1.4.6. □

The question which intuitively arises is how is a function from the Sobolev space defined on the boundary.

The boundary Γ of an n -dimensional domain Ω can be considered as an $(n - 1)$ -dimensional manifold. For the case $n = 1$ one gets zero-dimensional manifold which consists of distinct points. In that case, Sobolev inequality can be used to obtain conditions under which point values are well defined for functions in the Sobolev space. Furthermore, restrictions $u|_{\Gamma}$ of functions u from Sobolev spaces to manifolds of dimension $n - 1$ are used for the higher dimensional cases. Also, one should use the Lipschitz domain and Lipschitz boundary. For the smooth boundary and $u \in W^{1,p}(\Omega)$, the restriction to the boundary can be considered as a function in $L^p(\Gamma)$, whenever $1 \leq p \leq \infty$, but it does not guarantee that pointwise values of u on Γ will make sense. If $p = 2$, then by the definition, the restriction $u|_{\Gamma}$ is square integrable on Γ . Using this property one can define space $W_0^{m,p}(\Omega)$, that is the subset of $W^{m,p}(\Omega)$, as

$$W_0^{m,p}(\Omega) = \{u \in W^{m,p}(\Omega) : D^\alpha u|_\Gamma = 0 \text{ in } L^2(\Gamma), |\alpha| < m\}. \quad (14)$$

This restriction is often called the trace map. It is denoted by γ and it is defined on a Lipschitz domain Ω as a continuous linear map $\gamma : W^{1,p}(\Omega) \rightarrow L^p(\Gamma)$ such that if $u \in C(\bar{\Omega}) \cap W^{1,p}(\Omega)$ its image γu is well-defined function on Γ .

Another important inequality that should be introduced is Poincaré inequality. It is also called Friedrichs inequality. In order to do that, the space $H_0^1(\Omega)$ should be defined first.

For the standard Sobolev space $W^{m,p}(\Omega)$, in the case of $p = 2$, one gets the space $W^{m,2}(\Omega)$. This Sobolev space is denoted by $H^m(\Omega)$ and consequently, space $W_0^{m,2}(\Omega)$ is denoted by $H_0^m(\Omega)$. It can be defined as

$$H^m(\Omega) = \{u : D^\alpha u \in L^2(\Omega) : \forall \alpha \text{ such that } |\alpha| \leq m\}. \quad (15)$$

Also, it is a Hilbert space with the inner product

$$(u, v)_{H^m(\Omega)} = \sum_{|\alpha| \leq m} (D^\alpha u, D^\alpha v)_{L^2(\Omega)} = \sum_{|\alpha| \leq m} \int_\Omega D^\alpha u \overline{D^\alpha v} dx. \quad (16)$$

The corresponding norm is

$$\|u\|_{H^m(\Omega)} = \left(\sum_{|\alpha| \leq m} \|D^\alpha u\|_{L^2(\Omega)}^2 \right)^{\frac{1}{2}} = [(u, u)_{H^m(\Omega)}]^{\frac{1}{2}} < \infty. \quad (17)$$

The space $H_0^1(\Omega)$ is the space of all functions $u \in L^2(\Omega)$ which have all their first order derivatives in $L^2(\Omega)$ and their trace vanishes at the boundary. It is an important space used in the theory of boundary value problems. Finally, the Poincaré inequality can be introduced.

Proposition 2.1. (Poincaré inequality) Let $\Omega \subset \mathbb{R}^n$ be a bounded Lipschitz domain, then there exists a constant $C_P > 0$ such that

$$\|u\|_{H^1(\Omega)} \leq C_P \|\nabla u\|_{L^2(\Omega)}, \quad \forall u \in H_0^1(\Omega). \quad (18)$$

Proof. The proof can be found in [DD12], Proposition 5.28. \square

Here, the Poincaré inequality is defined on $H_0^1(\Omega)$, but there also exists a generalized version of it. For that, the term seminorm has to be introduced.

For a non-negative integer m and $u \in W^{m,p}(\Omega)$, the seminorm on $W^{m,p}(\Omega)$ is defined as

$$|u|_{W^{m,p}(\Omega)} = \left(\sum_{|\alpha|=m} \|D^\alpha u\|_{L^p(\Omega)}^p \right)^{\frac{1}{p}}, \quad 1 \leq p < \infty, \quad (19)$$

$$|u|_{W^{m,\infty}(\Omega)} = \max_{|\alpha|=m} \|D^\alpha u\|_{L^\infty(\Omega)}, \quad p = \infty. \quad (20)$$

It has all properties of a norm, except that $|u|_{W^{m,p}} = 0$ does not imply $u = 0$ in $W^{m,p}(\Omega)$. If Ω is bounded then $|\cdot|_{W^{m,p}(\Omega)}$ is a norm on $W_0^{m,p}(\Omega)$ equivalent to the usual norm $\|\cdot\|_{W^{m,p}(\Omega)}$.

Proposition 2.2. (Generalized Poincaré inequality) Let $\Omega \subset \mathbb{R}^n$ be a bounded Lipschitz domain, $1 \leq p < \infty$ and let \mathcal{N} be a continuous seminorm on $W^{1,p}(\Omega)$, i.e., a norm on the constants. Then there exists a constant $C > 0$ that depends on Ω , n , p such that

$$\|u\|_{W^{1,p}(\Omega)} \leq C \left(\left(\int_{\Omega} |\nabla u(x)|^p dx \right)^{\frac{1}{p}} + \mathcal{N}(u) \right), \quad \forall u \in W^{1,p}(\Omega). \quad (21)$$

Proof. The proof can be found in [DD12], Proposition 5.55. □

The Sobolev spaces $W^{m,p}(\Omega)$ can also be defined for negative integers m . The definition is based on the duality of Banach spaces. The dual space of the Lebesgue space $L^p(\Omega)$ can be easily defined through Hölder's inequality. Let p be in the range $1 < p < \infty$ and let q be the dual index to p , i.e., $\frac{1}{q} + \frac{1}{p} = 1$. Thus, space $L^q(\Omega)$ is a dual space of $L^p(\Omega)$. The space $L^p(\Omega)$ is reflexive if and only if $1 < p < \infty$. The dual of $L^\infty(\Omega)$ is larger than $L^1(\Omega)$. Therefore for space $L^1(\Omega)$ and $L^\infty(\Omega)$, this does not hold. The dual space of the Sobolev space $W^{m,p}(\Omega)$ is defined as $(W_0^{-m,q}(\Omega))'$ where q is the dual index to p . Also, a negative Sobolev space $H^{-m}(\Omega)$ is defined as $H^{-m}(\Omega) = (H_0^m(\Omega))'$.

2.2 Model problem

A model problem on which the finite element method will be developed is introduced in this section following [Ver13], [BS08], [Che05], and [LB13].

The domain Ω is defined as a connected, bounded and polygonal set in 2-dimensional real Euclidean space \mathbb{R}^2 . The boundary Γ consists of two disjoint parts: Γ_D (Dirichlet boundary) and Γ_N (Neumann boundary). Functions f and g belong to the spaces $L^2(\Omega)$ and $L^2(\Gamma_N)$, respectively. The focus is on linear second order elliptic equations with the Poisson equation as the main model problem. Thus, the model problem is called the Poisson equation with Dirichlet-Neumann boundary conditions and it is defined as

$$-\Delta u = f \text{ in } \Omega, \quad (22)$$

$$u = 0 \text{ on } \Gamma_D, \quad (23)$$

$$n \cdot \nabla u = g \text{ on } \Gamma_N. \quad (24)$$

Naturally, one wants to find a solution u of a given problem. Sometimes, this problem can be solved analytically, but usually, it is hard or even impossible to find u in that way. Therefore, a numerical technique for solving a differential equation should be used. The first step is to rewrite the differential equation as a variational equation. Before doing that, the question that arises is how to define a proper space.

Following the notation defined in [Ver13], the test space $H_D^1(\Omega)$ is the Sobolev space of functions from $H^1(\Omega)$ whose trace vanishes on the Dirichlet part of the boundary:

$$H_D^1(\Omega) = \{\phi \in H^1(\Omega) : \phi = 0 \text{ on } \Gamma_D\}. \quad (25)$$

As mentioned in a previous subsection, the space $H_D^1(\Omega)$ is a Hilbert space.

To get a variational formulation of the model problem, one should multiply (22) by a test function $v \in H_D^1(\Omega)$ and integrate over domain Ω . Furthermore, using Green's formula one obtains:

$$\begin{aligned}
\int_{\Omega} f v dx &= - \int_{\Omega} \Delta u v dx \\
&= \int_{\Omega} \nabla u \cdot \nabla v dx - \int_{\Gamma_D} n \cdot \nabla u v ds - \int_{\Gamma_N} n \cdot \nabla u v ds \\
&= \int_{\Omega} \nabla u \cdot \nabla v dx - \int_{\Gamma_N} n \cdot \nabla u v ds \\
&= \int_{\Omega} \nabla u \cdot \nabla v dx - \int_{\Gamma_N} g v ds.
\end{aligned}$$

In the penultimate line, the integral on a Dirichlet part of the boundary vanishes due to the assumption $v = 0$ on Γ_D .

The solution of the Poisson's equation is also the solution of the variational formulation. The converse is usually not true, because the solution of the variational formulation does not need to be two times differentiable. For this reason, it is also called the weak formulation. It is called variational because the function v can vary arbitrarily.

Thus, a variational formulation of the boundary value problem (22)-(24) is: find $u \in H_D^1(\Omega)$ such that

$$a(u, v) = \int_{\Omega} \nabla u \cdot \nabla v = \int_{\Omega} f v + \int_{\Gamma_N} g v = f(v) \quad (26)$$

for all $v \in H_D^1(\Omega)$.

The following fundamental theorem should be introduced to analyze this variational problem. The extension of the Riesz representation theorem (Theorem A.1) to non-symmetric bilinear forms is called the Lax-Milgram theorem.

Theorem 2.4. (Lax-Milgram theorem) *Given a Hilbert space V , a continuous, coercive bilinear form $a(\cdot, \cdot)$ and a continuous linear functional $f \in V'$, there exists a unique $u \in V$ such that*

$$a(u, v) = f(v) \quad \forall v \in V.$$

Proof. This proof can be found in [BS08], Theorem 2.7.7. □

Finally, the existence and uniqueness of the solution of the given variational problem (26) is provided by the following corollary and the property that $H_D^1(\Omega) \subset H_0^1(\Omega)$.

Corollary 2.2. *Let H be a Hilbert space, V a subspace of H . Let $a(\cdot, \cdot)$ be a coercive, continuous bilinear form on V , not necessarily symmetric. Then there exists a unique solution of the variational problem: given $f \in V'$, find $u \in V$ such that*

$$a(u, v) = f(v) \quad \forall v \in V.$$

Proof. The proof can be found in [BS08], Corollary 2.7.12. □

2.3 Conforming Finite Element discretization

The finite element method for the numerical solution of partial differential equations in two dimensions in its simplest form, i.e., conforming finite element method, will be introduced in this section. The used literature is [Ver13], [BS08], [Che05], [LB13], and [Cia91].

The finite element method is a process of constructing finite-dimensional subspaces $V_h \subset V$, which are then called the finite element spaces, consisting of piecewise polynomials over the finite element partition \mathcal{T}^h (i.e. mesh). The finite element method is called conforming because the space V_h is a subspace of the space V .

To begin with, one should transform the model problem into the variational formulation and then search for an approximate solution in the space of continuous piecewise functions. As defined before, $f \in V'$. The finite element approximation of variational problem means to find

$u_h \in V_h$ such that

$$a(u_h, v_h) = f(v_h) \quad (27)$$

for all $v_h \in V_h$.

It is called the Galerkin method for approximating the solution. If the bilinear form is symmetric, it is called the Ritz-Galerkin method. For both symmetric and non-symmetric forms, there exists a unique solution u_h that solves (27). It is because subset V_h is also a Hilbert space, then the existence and uniqueness are implied by using either the Riesz Representation theorem or the Lax-Milgram theorem.

Furthermore, it can be shown how problem (27) is solved. The choice of a proper basis of the space V_h is an important step. Let $(w_i)_{i=1}^N$ be the basis of space V_h , where N is the dimension of V_h . Then the solution of the problem (27) can be written as

$$u_h = \sum_{i=1}^N \varphi_i w_i$$

where the vector $(\varphi_1, \varphi_2, \dots, \varphi_N)$ is the solution of the linear system

$$\sum_{i=1}^N a(w_i, w_j) \varphi_i = f(w_j), \quad 1 \leq j \leq N. \quad (28)$$

The matrix A whose entries are $a(w_i, w_j)$ is called the stiffness matrix and the vector b where $b_j = f(w_j)$ is called the load vector. A stiffness matrix is always invertible and inherits properties of a bilinear form $a(\cdot, \cdot)$.

The question which arises is how to define subspace V_h of space V where V is usually defined as one of the Hilbert spaces $H_0^1(\Omega)$, $H^1(\Omega)$, $H_0^2(\Omega)$... Therefore, some properties are established in order to define it.

First of all, one should define triangulation \mathcal{T}^h over the set $\bar{\Omega}$. It is a decomposition of the set $\bar{\Omega}$ into a finite number of subsets K such that the following conditions are satisfied. To start with, $\bar{\Omega}$ can be defined as $\bar{\Omega} = \bigcup_{K \in \mathcal{T}^h} K$. Furthermore, for each $K \in \mathcal{T}^h$, the set K is closed and its interior $\overset{\circ}{K}$ is non-empty and connected, and the boundary Γ is Lipschitz-continuous. Also, for each distinct $K_1, K_2 \in \mathcal{T}^h$ it holds $\overset{\circ}{K}_1 \cap \overset{\circ}{K}_2 = \emptyset$. Since straight finite elements will be considered, i.e., finite elements that are all polyhedra in \mathbb{R}^n , $n \in \{2, 3\}$, another condition should be added. Any face of any element K_1 in the triangulation is

either a subset of the boundary Γ or a face of another element K_2 in the triangulation. In other words, an intersection of any two elements of triangulation is either empty or a common face. After the triangulation process is done, one obtains a finite-dimensional space V_h of functions defined over the set $\bar{\Omega}$.

Let P_K be the space defined as $P_K = \{v_h|_K : v_h \in V_h\}$. The functions $v_h \in V_h$ are piecewise polynomials such that for each $K \in \mathcal{T}^h$ the space P_K consists of polynomials. Let $\{\theta_j\}_{j=1}^n$ be the basis of the space P_K , where $n = \dim(P_K)$. The basis functions θ_j are called the shape functions. By taking a linear combination of them and coefficients, one obtains a polynomial function in P_K for each polygon K . The linear functionals $\Phi_i(\cdot)$, $i = 1, \dots, n$ are specifying the shape functions. A necessary compatibility condition for $\Phi_i(\cdot)$, K and P_K is called unisolvency. Unisolvency is defined in the sense that for any given real scalars a_i , $1 \leq i \leq n$, there exists a unique function $p \in P_K$ that satisfies

$$\Phi_i(p) = a_i, \quad 1 \leq i \leq n.$$

Also, calculation of the shape functions is done by solving the linear system

$$\Phi_i(\theta_j) = \delta_{ij}, \quad i, j = 1, \dots, n.$$

Functionals determine both the local and the global properties of the finite element space V_h . As mentioned before, functionals specify the shape functions on each $K \in \mathcal{T}^h$ but also, they can extend their influence on the behaviour of these shape functions outside of the polygon K , on adjacent polygons or even on the whole mesh \mathcal{T}^h .

Furthermore, the computation of the coefficients of the linear system (28) is preferably done on a reference finite element. Since simplicial finite elements are discussed, one can consider the reference triangle $\{x \in \mathbb{R}^2 : x_1 \geq 0, x_2 \geq 0, x_1 + x_2 \leq 1\}$ or the reference square $[0, 1]^2$, denoted by \hat{K} . Also, $R_1(\hat{K}) = \text{span}\{1, x_1, x_2\}$ is defined for the reference triangle or $R_1(\hat{K}) = \text{span}\{1, x_1, x_2, x_1x_2\}$ for the reference square.

Let $F_K : \hat{K} \rightarrow K$ be an affine diffeomorphism. Then every element $K \in \mathcal{T}^h$ is the image of the reference element \hat{K} under F_K . Therefore, one can define set $R_1(K) = \{\phi \circ F_K^{-1} : \phi \in R_1(\hat{K})\}$. The lowest order conforming finite element space associated with \mathcal{T}^h is

$$S^{1,0}(\mathcal{T}^h) = \{\phi \in C(\Omega) : \phi|_K \in R_1(K) \text{ for all } K \in \mathcal{T}^h\},$$

or if a boundary condition is used, then

$$S_D^{1,0}(\mathcal{T}^h) = \{\phi \in S^{1,0}(\mathcal{T}^h) : \phi = 0 \text{ on } \Gamma_D\}.$$

Finally, the finite element discretization of a problem (26) can be written as: Find $u_{\mathcal{T}^h} \in S_D^{1,0}(\mathcal{T}^h)$ such that:

$$\int_{\Omega} \nabla u_{\mathcal{T}^h} \cdot \nabla v_{\mathcal{T}^h} = \int_{\Omega} f v_{\mathcal{T}^h} + \int_{\Gamma_N} g v_{\mathcal{T}^h} \quad (29)$$

holds for all $v_{\mathcal{T}^h} \in S_D^{1,0}(\mathcal{T}^h)$.

The Lax-Milgram theorem (Theorem 2.4) implies a unique solution of the problem (29).

2.4 A priori estimate of the error in the L^2 norm of gradient

The goal of this section is to introduce an a priori error estimate for conforming finite element discretization, between the solution u of the original problem and the solution u_h of the discrete problem. The used literature is [GB05], [Cia91], [BS08], [LB13], [ESW05] and [EG04].

An error estimate is an expression that represents an approximation to the actual unknown error. There are two types of error estimation procedures, a priori and a posteriori. A posteriori error estimators are discussed in Chapter 3. A priori error estimates are used to get useful information on the asymptotic behavior of the discretization errors. They involve the unknown solution u , thus they are not computable.

To start with, the basic equation for error is derived by subtracting $a(u_h, v)$ from the weak formulation. Therefore one gets

$$\begin{aligned} a(u, v) - a(u_h, v) &= f(v) - a(u_h, v) \\ a(u - u_h, v) &= f(v) - a(u_h, v), \quad \forall v \in V. \end{aligned} \quad (30)$$

Restricting the test functions to the space V_h and using (27) one obtains the Galerkin orthogonality property, i.e., for any $w_h \in V_h$ it follows $a(u - u_h, w_h) = 0$. Furthermore, assume that $\|u - v_h\| < \|u - u_h\|$ with $v_h = u_h + w_h$ and $w_h \neq 0$. Then, by a straightforward calculation and using the Galerkin orthogonality one obtains $\|u - v_h\|^2 = \|u - u_h\|^2 + \|w_h\|^2$. Since $w_h \neq 0$ and $\|w_h\| > 0$, it follows that $\|u - v_h\|^2 < \|u - u_h\|^2$. Therefore, another property that arises is the best approximation property

$$a(u - u_h, u - u_h) = \inf_{v_h \in V_h} a(u - v_h, u - v_h). \quad (31)$$

As mentioned before, the bilinear form $a(\cdot, \cdot)$ is an inner product associated with the norm $\|u\|_V = \sqrt{a(u, u)}$, thus the above mentioned equation (31) can be written as

$$\|u - u_h\|_V = \inf_{v_h \in V_h} \|u - v_h\|_V. \quad (32)$$

Equation (32) states that the finite element solution is the best approximation result with respect to $\|\cdot\|_V$, i.e., there is no better approximation result in V_h . Because of the Galerkin orthogonality, the error $u - u_h$ is orthogonal to the space V_h , i.e., u_h is the projection of the solution u over V_h with the respect to $\|\cdot\|_V$.

An upper bound of the best approximation error is the interpolation error. Thus, it is more convenient to use the interpolation theory.

For introduction, the error estimate is established using the approximation space P_1 of piecewise linear functions.

Given a continuous function u , the Lagrangian piecewise linear interpolant is denoted by $I_h^1 u$. It satisfies $I_h^1 u(x_i) = u(x_i)$ at every vertex x_i of the triangulation. It is a well-defined function in V_h . Also, u is assumed to be two times weakly differentiable. Taking $v_h = I_h^1 u$ one wants to estimate the norm of the interpolation error $u - I_h^1 u$. The error can be represented as the sum of elementwise error bounds which are calculated in the norm defined on every

$K \in \mathcal{T}^h$. The case for the L^2 -norm of the gradient is

$$\|\nabla(u - I_h^1 u)\|_{L^2(\Omega)}^2 = \sum_{K \in \mathcal{T}^h} \|\nabla(u - I_h^1 u)\|_{L^2(K)}^2. \quad (33)$$

Thus, the problem of finding an estimate for the overall error is reduced to the problem of evaluating local interpolation estimates. The idea is to map the local interpolation error onto the reference element \hat{K} , apply the estimate on \hat{K} , and transform back to K . One obtains that through the following bounds. The first one is

$$\|\nabla(u - I_h^1 u)\|_{L^2(K)}^2 \leq 2 \frac{h_K^2}{|K|} \|\nabla(\hat{u} - I_h^1 \hat{u})\|_{L^2(\hat{K})}^2,$$

where $|K|$ is the area of element K and $\frac{h_K^2}{|K|}$ is the triangle aspect ratio. The second bound is a special case of the Bramble–Hilbert lemma (Lemma A.2), a lemma that is used as a general estimate for the interpolation error. One obtains

$$\|\nabla(\hat{u} - I_h^1 \hat{u})\|_{L^2(\hat{K})} \leq C \|D^2(\hat{u} - I_h^1 \hat{u})\|_{L^2(\hat{K})} = C \|D^2 \hat{u}\|_{L^2(\hat{K})}.$$

The third bound is

$$\|D^2 \hat{u}\|_{L^2(\hat{K})}^2 \leq 18 h_K^2 \frac{h_K^2}{|K|} \|D^2 u\|_{L^2(K)}^2.$$

One can find more information and intermediate steps in [ESW05, Chapter 1].

The following interpolation error estimates hold for any $K \in \mathcal{T}^h$.

Theorem 2.5. *The interpolant $I_h^1 u$ satisfies the estimates*

$$\begin{aligned} \|u - I_h^1 u\|_{L^2(K)} &\leq C h_K^2 \|D^2 u\|_{L^2(K)}, \\ \|D(u - I_h^1 u)\|_{L^2(K)} &\leq C h_K \|D^2 u\|_{L^2(K)}. \end{aligned} \quad (34)$$

Proof. More details in [LB13], Proposition 3.1. \square

Finally, with the help of the interpolation error, one finds that the error satisfies the following theorem.

Theorem 2.6. [LB13][Theorem 4.8.] *Let $a(\cdot, \cdot)$ be an inner product on V . The finite element solution u_h satisfies the estimate*

$$\|\nabla(u - u_h)\|_{L^2(\Omega)}^2 \leq C \sum_{K \in \mathcal{T}^h} h_K^2 \|D^2 u\|_{L^2(K)}^2.$$

Proof. Let $v_h = I_h^1 u$ in the best approximation result (32). Furthermore, using the interpolation error estimate (Theorem 2.5), one obtains

$$\begin{aligned} \|\nabla(u - u_h)\|_{L^2(\Omega)}^2 &\leq \|\nabla(u - I_h^1 u)\|_{L^2(\Omega)}^2 \\ &= \sum_{K \in \mathcal{T}^h} \|D(u - I_h^1 u)\|_{L^2(K)}^2 \\ &\leq \sum_{K \in \mathcal{T}^h} C h_K^2 \|D^2 u\|_{L^2(K)}^2, \end{aligned}$$

thus the estimate is proven. \square

Also, for the diameter h_K , i.e., the length of the longest edge of $K \in \mathcal{T}^h$, one gets $h_K \leq h$ for all triangles $K \in \mathcal{T}^h$. Therefore one can derive a bound that is independent of the local mesh width. Hence, from Theorem 2.6, it follows

$$\|\nabla(u - u_h)\|_{L^2(\Omega)}^2 \leq Ch^2 \sum_{K \in \mathcal{T}^h} \|D^2 u\|_{L^2(K)}^2 = Ch^2 \|D^2 u\|_{L^2(\Omega)}^2. \quad (35)$$

One can conclude that the gradient of the error tends to zero as the mesh size h tends to zero and the convergence order is at least 1.

The error estimate (35) was established using approximation space P_1 of piecewise linear functions. For other cases, the following definitions are presented.

Let $\hat{P}(\hat{K})$ be a polynomial space of dimension n_s , $\{\hat{\Phi}_i\}_{i=1}^{n_s}$ linear functionals and $\{\hat{\theta}_i\}_{i=1}^{n_s}$ the local basis of $\hat{P}(\hat{K})$. The local interpolation operator $I_{\hat{K}} \hat{v} \in \hat{P}(\hat{K})$ is defined as

$$I_{\hat{K}} \hat{v} = \sum_{i=1}^{n_s} \hat{\Phi}_i(\hat{v}) \hat{\theta}_i. \quad (36)$$

The domain of the interpolation operator is $V(\hat{K})$. Usually, it is assumed to be of the form $C^s(\hat{K})$ for some integer $s \geq 0$.

For all $K \in \mathcal{T}^h$, one must define a linear bijective mapping $\psi_K : V(K) \rightarrow V(\hat{K})$ to get \mathcal{T}^h -based finite elements. In this case, K is defined as $K = F_K(\hat{K})$ and $P_K = \{\psi_K^{-1}(\hat{p}); \hat{p} \in \hat{P}(\hat{K})\}$. Also, functionals are $\Phi_{K,i}(p) = \hat{\Phi}(\psi_K(p))$, $\forall p \in P_K$ and basis functions are $\theta_{K,i} = \psi_K^{-1}(\hat{\theta}_i)$, $1 \leq i \leq n_s$. Therefore, the local interpolation operator $I_K v \in P_K$ is

$$I_K v = \sum_{i=1}^{n_s} \Phi_{K,i}(v) \theta_{K,i}. \quad (37)$$

Due to the linearity of ψ_K , a property that is important for the analysis of the interpolation error, it is

$$I_{\hat{K}}(\psi_K(v)) = \sum_{i=1}^{n_s} \hat{\Phi}_i(\psi_K(v)) \hat{\theta}_i = \sum_{i=1}^{n_s} \Phi_{K,i}(v) \psi_K(\theta_{K,i}) = \psi_K(I_K(v)). \quad (38)$$

The global interpolation operator $I_h v$ can be described elementwise using the local interpolation operators (37), i.e.,

$$\forall K \in \mathcal{T}^h, (I_h v)|_K = I_K(v|_K) = \sum_{i=1}^{n_s} \Phi_{K,i}(v|_K) \theta_{K,i}.$$

Furthermore, one wants to estimate the norm of the interpolation error $v - I_h v$ with the interpolation operator defined as (37). The diameter of the largest ball inscribed in $K \in \mathcal{T}^h$ is denoted by ρ_K . The affine mapping F_K is defined as $F_K \hat{x} = B_K \hat{x} + b$ where B_K is a non-singular $n \times n$ matrix and b is a n vector. If $\|\cdot\|$ is the matrix norm, then it holds

$$\|B_K\| \leq \frac{h_K}{\rho_K} \text{ and } \|B_K^{-1}\| \leq \frac{h_{\hat{K}}}{\rho_K}. \quad (39)$$

Mappings $\psi_K : V(K) \rightarrow V(\hat{K})$ are set as $\psi_K(v) = \hat{v} = v \circ F_K$. The following lemma will be used in the proof of Theorem 2.7.

Lemma 2.1. Let $s \geq 0$ and let $1 \leq p \leq \infty$. There exists c such that, for all K and $w \in W^{s,p}(K)$,

$$\begin{aligned} \sum_{|\alpha|=s} \|D^\alpha \hat{w}\|_{L^p(\hat{K})} &\leq c \|B_K\|^s |\det(B_K)|^{-\frac{1}{p}} \sum_{|\alpha|=s} \|D^\alpha w\|_{L^p(K)}, \\ \sum_{|\alpha|=s} \|D^\alpha w\|_{L^p(K)} &\leq c \|B_K^{-1}\|^s |\det(B_K)|^{\frac{1}{p}} \sum_{|\alpha|=s} \|D^\alpha \hat{w}\|_{L^p(\hat{K})}, \end{aligned}$$

where $\hat{w} = w \circ F_K$. For any positive real x in the case when $p = \infty$, it is set $x^{\pm \frac{1}{p}} = 1$.

Proof. This proof can be found in [EG04], Lemma 1.101. \square

Theorem 2.7. [EG04][Theorem 1.103.] Let a family of finite elements be given by its reference cell \hat{K} , the functionals $\{\hat{\Phi}_i\}$ and a space of polynomials $\hat{P}(\hat{K})$. Let $1 \leq p \leq \infty$ and assume that there exists an integer k such that $P_k \subset \hat{P}(\hat{K}) \subset W^{k+1,p}(\hat{K}) \subset V(\hat{K})$. Let $F_K : \hat{K} \rightarrow K$ be an affine bijective mapping and let I_K^k be the local interpolation operator on K defined in (37). Let $0 \leq l \leq k$ and $W^{l+1,p}(\hat{K}) \subset V(\hat{K})$ with continuous embedding. Then, setting $\sigma_K = \frac{h_K}{\rho_K}$, there exists $C > 0$ such that, for all $m \in \{0, \dots, l+1\}$ and $\forall K, \forall v \in W^{l+1,p}(K)$,

$$\sum_{|\alpha|=m} \|D^\alpha (v - I_K^k v)\|_{L^p(K)} \leq C h_K^{l+1-m} \sigma_K^m \sum_{|\alpha|=l+1} \|D^\alpha v\|_{L^p(K)}.$$

Proof. Let $I_{\hat{K}}^k$ be the local interpolation operator on \hat{K} defined in (36). Let $\hat{w} \in W^{l+1,p}(\hat{K})$ and let $\mathcal{F} : W^{l+1,p}(\hat{K}) \rightarrow W^{m,p}(\hat{K})$ be a linear operator defined as $\mathcal{F}\hat{w} = \hat{w} - I_{\hat{K}}^k \hat{w}$. Since $W^{l+1,p}(\hat{K}) \subset V(\hat{K})$ with continuous embedding, the linear operator \mathcal{F} is continuous from $W^{l+1,p}(\hat{K})$ to $W^{m,p}(\hat{K})$ for all $m \in \{0, \dots, l+1\}$. Since $l \leq k$, then $P_l \subset \hat{P}(\hat{K})$ and, therefore, P_l is invariant under $I_{\hat{K}}^k$. This holds because of the property of the local interpolation operator that $\hat{P}(\hat{K})$ is invariant under $I_{\hat{K}}^k$, i.e., $\forall \hat{p} \in \hat{P}(\hat{K}), I_{\hat{K}}^k \hat{p} = \hat{p}$. Hence, \mathcal{F} vanishes on P_l . As a consequence, and with using Deny-Lions Lemma (Lemma A.1), it follows

$$\begin{aligned} \sum_{|\alpha|=m} \|D^\alpha (\hat{w} - I_{\hat{K}}^k \hat{w})\|_{L^p(\hat{K})} &= \sum_{|\alpha|=m} \|D^\alpha \mathcal{F}(\hat{w})\|_{L^p(\hat{K})} \\ &= \inf_{\hat{p} \in P_l} \sum_{|\alpha|=m} \|D^\alpha \mathcal{F}(\hat{w} + \hat{p})\|_{L^p(\hat{K})} \\ &\leq \|\mathcal{F}\|_{\mathcal{L}(W^{l+1,p}(\hat{K}); W^{m,p}(\hat{K}))} \inf_{\hat{p} \in P_l} \sum_{|\alpha| \leq l+1} \|D^\alpha (\hat{w} + \hat{p})\|_{L^p(\hat{K})} \\ &\leq c \inf_{\hat{p} \in P_l} \sum_{|\alpha| \leq l+1} \|D^\alpha (\hat{w} + \hat{p})\|_{L^p(\hat{K})} \\ &\leq c \sum_{|\alpha|=l+1} \|D^\alpha \hat{w}\|_{L^p(\hat{K})}. \end{aligned}$$

Let $v \in W^{l+1,p}(K)$ and set $\hat{v} = \psi_K(v) = v \circ F_K$. From the property (38), it

follows $[I_K^k v] \circ F_K = I_{\hat{K}}^k \hat{v}$. Using Lemma 2.1 yields

$$\begin{aligned}
\sum_{|\alpha|=m} \|D^\alpha(v - I_K^k v)\|_{L^p(K)} &\leq c \|B_K^{-1}\|^m |\det(B_K)|^{\frac{1}{p}} \sum_{|\alpha|=m} \|D^\alpha(\hat{v} - I_{\hat{K}}^k \hat{v})\|_{L^p(\hat{K})} \\
&\leq c \|B_K^{-1}\|^m |\det(B_K)|^{\frac{1}{p}} \sum_{|\alpha|=l+1} \|D^\alpha \hat{v}\|_{L^p(\hat{K})} \\
&\leq c \|B_K^{-1}\|^m \|B_K\|^{l+1} \sum_{|\alpha|=l+1} \|D^\alpha v\|_{L^p(K)} \\
&\leq c (\|B_K\| \|B_K^{-1}\|)^m \|B_K\|^{l+1-m} \sum_{|\alpha|=l+1} \|D^\alpha v\|_{L^p(K)}.
\end{aligned}$$

With property (39) one can conclude the proof. \square

The following theorem is used to establish the error bounds with higher-order approximation space, i.e., P_m , $m \geq 2$.

Theorem 2.8. *Using a higher-order finite element approximation space P_m or Q_m with $m \geq 2$ leads to the higher-order convergence bound*

$$\|\nabla(u - u_h)\|_{L^2(\Omega)} \leq C_m h^m \|D^{m+1}u\|_{L^2(\Omega)}.$$

Proof. More details in [ESW05], Theorem 1.21. \square

In other words, one gets m -th order convergence as long as the regularity of the target solution is good enough. Also, remark that $\|D^{m+1}u\|_{L^2(\Omega)} < \infty$ if and only if the $(m+1)$ st generalized derivatives of u are in $L^2(\Omega)$.

2.5 Neumann and Dirichlet cases

The mixed Dirichlet-Neumann boundary conditions are presented in this section following [EG04] and [BS08].

A model problem (22)-(24), i.e., the Poisson equation with Dirichlet-Neumann boundary conditions, is considered on a bounded, polygonal, and connected domain Ω . As mentioned before, the boundary is $\Gamma = \Gamma_D \cup \Gamma_N$. A Dirichlet condition is defined on Γ_D and a Neumann condition on Γ_N . One can obtain homogeneous Dirichlet condition (23) from the case when the Dirichlet condition is non-homogeneous. To get that, assume that Γ_D is smooth enough. Then it is possible to define $H^{\frac{1}{2}}(\Gamma_D)$. One should remark that every function in $H^{\frac{1}{2}}(\Gamma)$ is the trace of a function in $H^1(\Omega)$, which follows from the statement (i) of the Theorem A.3. Furthermore, for all $g \in H^{\frac{1}{2}}(\Gamma_D)$, there exists an extension $\tilde{g} \in H^{\frac{1}{2}}(\Gamma)$ with properties $\tilde{g}|_{\Gamma_D} = g$ and $\|\tilde{g}\|_{H^{\frac{1}{2}}(\Gamma)} \leq c \|g\|_{H^{\frac{1}{2}}(\Gamma_D)}$ uniformly in g . Using the lifting of \tilde{g} in $H^1(\Omega)$ (Corollary A.1) one can assume that the Dirichlet condition is homogeneous. Therefore, the boundary conditions are defined as in (23)-(24). Taking the solution and the test function in the Sobolev space $H_D^1(\Omega)$, one obtains the weak formulation (26) by multiplying Poisson's equation by a test function, integrating over Ω and then integrating by parts. One concludes:

Proposition 2.3. Let $\Gamma_D \subset \Gamma$, assume $\text{meas}(\Gamma_D) > 0$, and set $\Gamma_N = \Gamma \setminus \Gamma_D$. Let $g \in L^2(\Gamma_N)$. If u solves (26), then $-\Delta u = f$ almost everywhere in Ω , $u = 0$ almost everywhere on Γ_D and $n \cdot \nabla u = g$ almost everywhere on Γ_N .

Proof. More details in [EG04], Proposition 3.6. □

Thus, mixed Dirichlet-Neumann boundary conditions formulate the weak problem. The equation and the boundary conditions are satisfied almost everywhere by the weak solution.

In the case when a model problem (22)-(24) has homogeneous Dirichlet and Neumann boundary conditions, the equations (22) and (24) are defined as $u = 0$ on Γ_D and $n \cdot \nabla u = 0$ on Γ_N , respectively. Then, the variational problem is defined as:

Proposition 2.4. Let $u \in H^2(\Omega)$ solve Poisson's equation (22) (this implies $f \in L^2(\Omega)$) with homogenous Dirichlet and Neumann boundary conditions. Then u can be characterized via $u \in H_D^1(\Omega)$ satisfies $a(u, v) = (f, v)$ for every $v \in H_D^1(\Omega)$.

Proof. The proof can be found in [BS08], Proposition 5.1.7. □

One should remark that the boundary term vanishes for $v \in H_D^1(\Omega)$ because either v or $n \cdot \nabla v$ is zero on any part of the boundary.

Proposition 2.5. [BS08][Proposition 5.1.9] Let $f \in L^2(\Omega)$ and suppose that $u \in H^2(\Omega)$ solves the variational equation. Then u solves Poisson's equation (22) with homogeneous Dirichlet and Neumann boundary conditions.

Proof. The Dirichlet boundary condition on u follows since $u \in H_D^1(\Omega)$. Using Green's formula (Definition 16), with $v \in C_0^\infty(\Omega) \subset H_D^1(\Omega)$ and $a(u, v) = (f, v)$, one gets

$$\int_{\Omega} (f + \Delta u)v dx = (f, v) - \int_{\Omega} \nabla u \cdot \nabla v dx = (f, v) - a(u, v) = 0.$$

Since $C_0^\infty(\Omega)$ is dense in $L^2(\Omega)$ (Corollary 2.1), the differential equation (22) is satisfied in $L^2(\Omega)$. Also, Green's formula then implies that

$$0 = (f, v) - a(u, v) = \int_{\Omega} (-\Delta u)v dx - \int_{\Omega} \nabla u \cdot \nabla v dx = \int_{\Gamma} n \cdot \nabla u v ds$$

for all $v \in H_D^1(\Omega)$. The Neumann boundary condition on u follows if $v|_{\Gamma_N}$ can be chosen arbitrarily with $v \in H_D^1(\Omega)$. Let U and U' be defined as in the Definition 11, and let Γ fulfill conditions a) and b) of the Definition 11. In other words, in a neighbourhood of x , Ω is below the graph of φ and the boundary Γ is the graph of φ . Since it is assumed that Γ is Lipschitz boundary and Γ_D a closed subset of it, this means that for any point $x \in \Gamma_N$ there is a neighbourhood U of x such that $\Gamma \cap U$ can be written as a graph of a Lipschitz function φ . Therefore, $\Gamma \cap U$ is defined as $\Gamma \cap U = \{y = (y', y_n) \in U: y_n = \varphi(y')\}$. Also, one has that

$$\Omega \cap U = \{y = (y', y_n) \in U: y_n < \varphi(y')\}.$$

The boundary integral over $\Gamma \cap U$ can be written as

$$\int_{\Gamma \cap U} n \cdot \nabla uv ds = \int_{U'} (n \cdot \nabla uv)(y', \varphi(y')) \sqrt{1 + |\nabla \varphi(y')|^2} dy'.$$

Let $w \in C_0^\infty(U')$ and set

$$v(y', t + \varphi(y')) = w(y') \left(1 + \frac{t}{a_i}\right) \quad \forall y' = (y_1, y_2, \dots, y_{n-1}) \in U', \quad -a_i < t < 0$$

where v is defined to be zero elsewhere. Then it follows that $v \in H_D^1(\Omega)$ and

$$0 = \int_{\Gamma} n \cdot \nabla uv ds = \int_{\Gamma \cap U} n \cdot \nabla uv ds = \int_{U'} w(y') n \cdot \nabla u(y', \varphi(y')) \sqrt{1 + |\nabla \varphi(y')|^2} dy'.$$

The L^∞ function $\sqrt{1 + |\nabla \varphi(y')|^2}$ is bounded below by 1 and w was chosen arbitrary. Therefore, one concludes that $n \cdot \nabla u|_{\Gamma \cap U} = 0$. Since Γ_N is covered by neighborhoods U , one concludes that the Neumann condition holds on all of Γ_N . \square

Choose $g_N \in L^2(\Gamma_N)$ and $g_D \in H^1(\Omega)$. Although g_D is defined on Ω , only the trace on Γ_D is used, with the same symbol. In other words, there exists a lifting \tilde{g}_D of g_D in $H^1(\Omega)$. In the case when a model problem (22)-(24) has a non-homogeneous Dirichlet and Neumann boundary conditions, the equations (23) and (24) are defined as $u = g_D$ on Γ_D and $n \cdot \nabla u = g_N$ on Γ_N , respectively. Define the space $H_{g_D, D}^1(\Omega) = \{\phi \in H^1(\Omega) : \phi = g_D \text{ on } \Gamma_D\}$. Remark that the Dirichlet condition $u = g_D$ on Γ_D is built into the definition of the space $H_{g_D, D}^1(\Omega)$. On the other hand, functions in the space $H_D^1(\Omega)$ are zero on the Dirichlet part of the boundary. Any function u that satisfies Poisson's equation (22) with non-homogeneous Dirichlet and Neumann boundary conditions, is also a solution of the following continuous problem: find $u \in H_{g_D, D}^1(\Omega)$ such that

$$a(u, v) = (\nabla u, \nabla v) = (f, v) + \int_{\Gamma_N} g_N(s) v(s) ds,$$

for all $v \in H_D^1(\Omega)$. The solution space and the test space are different in this variational equation. Since Ω is a polygonal and bounded set, boundaries Γ_D and Γ_N also have a polygonal form. Then one can triangulate Ω in a way that the edges of Γ_D and Γ_N are composed of side faces of grid cells. Let P_1 be the space of the continuous, piecewise, linear finite elements of this triangulation with the property $v_h(V_i) = g_D(V_i)$ for all corner points $V_i \in \Gamma_D$. Let $P_{1,0}$ be the space of the continuous, piecewise, linear finite elements of this triangulation with the property $v_h(V_i) = 0$ for all corner points $V_i \in \Gamma_D$. The finite element method is defined by: find $u_h \in P_1$ so that

$$a(u_h, v_h) = (\nabla u_h, \nabla v_h) = (f, v_h) + \int_{\Gamma_N} g_N(s) v_h(s) ds \quad \forall v_h \in P_{1,0}.$$

If $g_N \neq 0$, the finite element equation has an additional contribution on the right-hand side of the system of equations that needs to be assembled. Therefore only the test functions that don't disappear on Γ_N are affected.

The convergence estimation starts as usual with the error equation, which is obtained by subtracting the finite element equation from the continuous equation

$$(\nabla(u - u_h), \nabla v_h) = 0 \quad \forall v_h \in P_{1,0}.$$

Since $I_h(u - u_h) \in P_{1,0}$, by applying this function in the error equation, $I_h u_h = u_h$ and Cauchy-Schwarz inequality, it follows:

$$\begin{aligned} \|\nabla(u - u_h)\|_{L^2(\Omega)}^2 &= (\nabla(u - u_h), \nabla(u - u_h) - \nabla(I_h(u - u_h))) \\ &= (\nabla(u - u_h), \nabla(u - I_h u_h)) \\ &\leq \|\nabla(u - u_h)\|_{L^2(\Omega)} \|\nabla(u - I_h u_h)\|_{L^2(\Omega)}. \end{aligned}$$

Due to the change of the boundary conditions, the solution of the continuous problem is not in $H^2(\Omega)$. Therefore the interpolation has a reduced order of convergence. In the case $d = 2$ and if the change of the boundary condition takes place on a straight line, the following error estimates are optimal:

$$\|\nabla(u - u_h)\|_{L^2(\Omega)} = c(u)h^{\frac{1}{2}}, \quad \|u - u_h\|_{L^2(\Omega)} = c(u)h.$$

Thus, only half of the order of convergence as with pure Dirichlet problems exists.

3 A Posteriori Error Estimators

3.1 Goals

The used literature in this section is [Ver13], [EG04], [ESW05] and [SS05].

A posteriori error estimates are one type of error estimation procedure. Their goal is to evaluate the error $u - u_h$ in terms of known data only, i.e., the size of the mesh cells, the approximation solution and the problem data. A posteriori error estimates are one of the main tools in the adaptive finite element method which is the main topic of this thesis.

The question which arises is when one should use adaptive methods. The motivation for using them is the fact that many physical problems of interest have singularities. Singularities appear from re-entrant corners or domains, interior or boundary layers, and sharp moving fronts. The overall accuracy of numerical approximations decreases when local singularities increase. The idea to fix further decreasing of approximations is to put more grid points where singularities occur. However, those regions should be carefully identified and one should find a good balance between refined and unrefined regions. Adaptive methods use information from earlier computations to locally refine the mesh. Therefore they automatically adjust themselves to improve approximations.

Another question that appears is how to establish good estimates of the accuracy of the computed solution. The answer is: with a posteriori error estimates. A priori error estimates are not sufficient in this case. They essentially provide only asymptotic information. On the other hand, a posteriori error estimates provide reliable upper and lower bounds for the error. A posteriori error estimates can be divided into several categories: residual estimates, hierarchical error estimates, averaging methods,... Here, the focus is on the residual estimates. They estimate the error of the numerical solution by a norm of its residual. In particular, a residual a posteriori error estimator $\eta_{R,K}$ is used for this purpose. It is extracted a posteriori from the computed solution. The adaptive method used in this thesis is based on the residual a posteriori error estimator $\eta_{R,K}$. Therefore the goals are to define it and to obtain upper and lower bounds for the error. An important requirement is that $\eta_{R,K}$ should be cheaper to compute than to compute the numerical solution. If $\eta_{R,K}$ provides a global upper bound on the error, then $\eta_{R,K}$ is reliable and the accuracy of the solution is below a tolerance. If $\eta_{R,K}$ provides a lower bound for the local error then the estimator $\eta_{R,K}$ is effective when it is used to drive an adaptive refinement process. An adaptive process will provide successive meshes that are correctly refined in the presence of the singularities.

Another question is how to correctly refine meshes. The location of the nodes depends on the geometry of the parental element, therefore on the structure of the initial coarse triangulation. First, the elements of the mesh have to be marked with the marking strategy. Then, they are either refined or coarsened by local refinement or coarsening based on error estimators. One can use the mesh smoothing process to optimize the placement of nodes. The goal is to obtain an optimal mesh where the number of unknowns is as small as possible to keep the error below the tolerance. This can be costly and one should try to minimize the cost. To sum up, an adaptive mesh-refinement process is presented through the general adaptive algorithm (Algorithm 3.1).

3.2 Adaptive algorithm

This section presents the general adaptive algorithm. The used literature is [Ver13], [D96] and [SS05].

The outline of the algorithm is, starting from an initial triangulation \mathcal{T}^{h_0} , a sequence of triangulations \mathcal{T}^{h_k} is obtained for $k = 1, 2, \dots$ until the estimated error is below the given tolerance ϵ using a minimal amount of work. Following [Ver13, Algorithm 1.1], a general algorithm for stationary problems is defined as follows:

Algorithm 3.1 (General adaptive algorithm). *Given the data of a partial differential equation and a tolerance ϵ as an input values, the goal is to provide a numerical solution with an error less than ϵ .*

- (1) *Construct an initial coarse mesh \mathcal{T}^{h_0} representing sufficiently well the geometry and data of the problem; set $k = 0$.*
- (2) *Solve the discrete problem associated with \mathcal{T}^{h_k} .*
- (3) *For every element $K \in \mathcal{T}^{h_k}$ compute the a posteriori error indicator.*
- (4) *If the estimated global error is less than ϵ stop, otherwise decide which elements have to be refined and construct the next mesh $\mathcal{T}^{h_{k+1}}$. Increase k by 1 and return to step (2).*

For points (1) and (2), one must specify a discretization method and a solution method for the discrete problems. It is assumed that the exact solutions of the finite dimensional problems can be obtained. For point (3) one estimates a posteriori error indicator for every element K . The upper estimate presents that error indicator can be used as a reliable stopping criterion for the algorithm, and the lower estimate proposes that an unnecessary work can be avoided. For step (4), having the set of local error estimates for all K , one needs an algorithm that uses this information to construct the next mesh $\mathcal{T}^{h_{k+1}}$. An required algorithm, i.e., refinement strategy, determines which elements have to be refined or coarsened and how to do that. The way these triangles are marked with marking strategies influences the efficiency of the whole Algorithm 3.1. Therefore, to make an algorithm operative, one needs to specify all of the above points.

After providing all the necessary data, the goal is to prove that an adaptive algorithm gives a sequence of discrete solutions that converges to the true solution of the differential equation. Chapter 4 proves the convergence of an adaptive algorithm.

3.3 Residual a posteriori error estimates

This section introduces one type of a posteriori error estimates called residual a posteriori error estimates. The residual estimates provide upper and lower bounds for the error of the discrete solution. The steps for obtaining bounds, as well as the residual a posteriori error indicator $\eta_{R,K}$ are presented. The used literature in this section is [Ver13], [GB05] and [Che05].

Let $u \in H_D^1(\Omega)$ and $u_{\mathcal{T}^h} \in S_D^{1,0}(\mathcal{T}^h)$ be the solutions of (26) and (29). The starting point is the error equation (30). Considering the model problem (22)-(24) and its variational formulation (26), (30) can be rewritten as

$$\int_{\Omega} \nabla(u - u_{\mathcal{T}^h}) \cdot \nabla v = \int_{\Omega} f v + \int_{\Gamma_N} g v - \int_{\Omega} \nabla u_{\mathcal{T}^h} \cdot \nabla v, \quad \forall v \in H_D^1(\Omega).$$

The right-hand side implicitly defines the residual of $u_{\mathcal{T}^h}$. It is an element of the dual space of $H_D^1(\Omega)$, denoted by $\mathcal{R}(v)$, $\forall v \in H_D^1(\Omega)$.

There are several necessary steps needed to derive the a posteriori error estimates. To start with, since $S_D^{1,0}(\mathcal{T}^h) \subset H_D^1(\Omega)$, the Galerkin orthogonality of the error holds. For all $w_{\mathcal{T}^h} \in S_D^{1,0}(\mathcal{T}^h)$ it follows

$$\int_{\Omega} \nabla(u - u_{\mathcal{T}^h}) \cdot \nabla w_{\mathcal{T}^h} = 0, \text{ i.e., } R(w_{\mathcal{T}^h}) = 0.$$

Furthermore, one wants to show the equivalence of the norm of the error and a dual norm of the residual. Defining the L^2 -norm of the gradient of v as

$$\|\nabla v\|_{L^2(\Omega)} = \sup_{w \in H_D^1(\Omega) \setminus \{0\}} \frac{1}{\|\nabla w\|_{L^2(\Omega)}} \int_{\Omega} \nabla v \cdot \nabla w, \quad (40)$$

it follows

$$\|\nabla(u - u_{\mathcal{T}^h})\|_{L^2(\Omega)} = \sup_{w \in H_D^1(\Omega) \setminus \{0\}} \frac{\mathcal{R}(w)}{\|\nabla w\|_{L^2(\Omega)}}. \quad (41)$$

The supremum term in (41) is equal to the norm of the residual in the dual space of $H_D^1(\Omega)$. Therefore this equality implies that the norm in $H_D^1(\Omega)$ of the error is equal to the norm of the residual in the dual space of $H_D^1(\Omega)$.

Before proceeding to the next step, the following definitions and notations are introduced. Let \mathcal{E} be the set of all edges associated with a partition \mathcal{T}^h . Furthermore, let \mathcal{E}_{Ω} denote the set of all interior edges e and \mathcal{E}_{Γ} the set of all edges on Γ . Similarly, let \mathcal{E}_{Γ_D} be the set of edges e on Γ_D and \mathcal{E}_{Γ_N} be the set of edges e on Γ_N . The union of all edges in \mathcal{E} is denoted by Λ . With every edge e a unit vector \mathbf{n}_e is associated. For $e \in \mathcal{E}_{\Gamma}$ it is the outward unit normal to Γ . For $e \in \mathcal{E}_{\Omega}$ the direction of it is associated with the definition of jumps across e . For any piecewise continuous function v it holds

$$\mathcal{J}_e(v)(x) = \lim_{t \rightarrow 0^+} v(x - t\mathbf{n}_e) - \lim_{t \rightarrow 0^+} v(x + t\mathbf{n}_e), \forall x \in e.$$

The next step is to establish an L^2 -representation of the residual. Residual estimates contain weighted L^2 -norms of element and edge residuals. Element residuals are defined as $r|_K = f + \Delta u_{\mathcal{T}^h}$ on every $K \in \mathcal{T}^h$. Edge residuals are defined as

$$j|_e = \begin{cases} -\mathcal{J}_e(\mathbf{n}_e \cdot \nabla u_{\mathcal{T}^h}), & \text{if } e \in \mathcal{E}_{\Omega}, \\ g - \mathbf{n}_e \cdot \nabla u_{\mathcal{T}^h}, & \text{if } e \in \mathcal{E}_{\Gamma_N}, \\ 0, & \text{if } e \in \mathcal{E}_{\Gamma_D}. \end{cases} \quad (42)$$

In the following lines, \mathbf{n}_K denotes the unit outward normal to the element K . Also, remark that $\Delta u_{\mathcal{T}^h} = 0$ on all triangles. Integration by parts element-wise and rearranging terms leads to

$$\begin{aligned}
R(w) &= \int_{\Omega} fw + \int_{\Gamma_N} gw + \sum_{K \in \mathcal{T}^h} \left\{ \int_K \Delta u_{\mathcal{T}^h} w - \int_{\partial K} \mathbf{n}_K \cdot \nabla u_{\mathcal{T}^h} w \right\} \\
&= \sum_{K \in \mathcal{T}^h} \int_K (f + \Delta u_{\mathcal{T}^h}) w + \sum_{e \in \mathcal{E}_{\Gamma_N}} \int_e (g - \mathbf{n}_e \cdot \nabla u_{\mathcal{T}^h}) w \\
&\quad - \sum_{e \in \mathcal{E}_{\Omega}} \int_e \mathcal{J}_e(\mathbf{n}_e \cdot \nabla u_{\mathcal{T}^h}) w \\
&= \int_{\Omega} rw + \int_{\Lambda} jw, \quad \forall w \in H_D^1(\Omega). \tag{43}
\end{aligned}$$

The next step is an error estimate for an interpolant $I_{\mathcal{T}^h} w$. First of all, the set of all vertices associated with a partition \mathcal{T}^h is denoted by \mathcal{N} and sets \mathcal{N}_{Ω} , \mathcal{N}_{Γ_N} are defined for vertices analogously as they are defined for the sets of edges \mathcal{E}_{Ω} , \mathcal{E}_{Γ_N} . The interpolant is defined as

$$I_{\mathcal{T}^h} w = \sum_{n \in \mathcal{N}_{\Omega} \cup \mathcal{N}_{\Gamma_N}} w_{K_n} \lambda_n.$$

Here, w_{K_n} is the average of w on K_n , i.e., the average of w on the union of all elements having n as a vertex. $\lambda_n \in S^{1,0}(\mathcal{T}^h)$ is a nodal shape function of a vertex $n \in \mathcal{N}$ that gives values $\lambda_n(n) = 1$, $\lambda_n(x) = 0$, $\forall x \in \mathcal{N} \setminus \{n\}$. Utilizing the Galerkin orthogonality condition into (43) and choosing $w_{\mathcal{T}^h} = I_{\mathcal{T}^h} w$ for $w \in H_D^1(\Omega)$ results in

$$R(w) = \sum_{K \in \mathcal{T}^h} \int_K r(w - I_{\mathcal{T}^h} w) + \sum_{e \in \mathcal{E}} \int_e j(w - I_{\mathcal{T}^h} w). \tag{44}$$

Furthermore, the shape regularity is another condition that partition \mathcal{T}^h has to satisfy, i.e., for any element K , the ratio $\frac{h_K}{\rho_K}$ is bounded independently of K . The shape parameter of \mathcal{T}^h , defined as $\sigma_{\mathcal{T}^h} = \max_{K \in \mathcal{T}^h} \frac{h_K}{\rho_K}$, must be bounded uniformly with respect to all partitions derived by local or global refinement. Let \tilde{K}_n and \tilde{K}_e denote the unions of all elements that share at least a vertex with a given element K or edge e , respectively. Let c_1 and c_2 be the interpolation constants that depend, for the used model problem, on the shape parameter. According to the interpolation theory, one has

$$\|v - I_{\mathcal{T}^h} v\|_{L^2(K)} \leq c_1 h_K \|\nabla v\|_{L^2(\tilde{K}_n)}, \tag{45}$$

$$\|v - I_{\mathcal{T}^h} v\|_{L^2(e)} \leq c_2 h_e^{\frac{1}{2}} \|\nabla v\|_{L^2(\tilde{K}_e)}. \tag{46}$$

Applying the Cauchy–Schwarz inequality element-wise on (44) and using results of interpolation theory (45, 46) yields

$$R(w) \leq \sum_{K \in \mathcal{T}^h} \|r\|_{L^2(K)} \|w - I_{\mathcal{T}^h} w\|_{L^2(K)} + \sum_{e \in \mathcal{E}} \|j\|_{L^2(e)} \|w - I_{\mathcal{T}^h} w\|_{L^2(e)} \tag{47}$$

$$\leq \sum_{K \in \mathcal{T}^h} \|r\|_{L^2(K)} c_1 h_K \|\nabla w\|_{L^2(\tilde{K}_n)} + \sum_{e \in \mathcal{E}} \|j\|_{L^2(e)} c_2 h_e^{\frac{1}{2}} \|\nabla w\|_{L^2(\tilde{K}_e)}. \tag{48}$$

Using the above estimates, the Cauchy-Schwarz inequality for sums and the properties of the shape regularity leads to

$$R(w) \leq \max\{c_1, c_2\} \sigma_{\mathcal{T}^h} \|\nabla w\|_{L^2(\Omega)} \left\{ \sum_{K \in \mathcal{T}^h} h_K^2 \|r\|_{L^2(K)}^2 + \sum_{e \in \mathcal{E}} h_e \|j\|_{L^2(e)}^2 \right\}^{\frac{1}{2}}.$$

Finally, defining $c^* = \max\{c_1, c_2\} \sigma_{\mathcal{T}^h}$ and combining the above estimates with (41) one can bound the error $\|\nabla(u - u_{\mathcal{T}^h})\|_{L^2(\Omega)}$ from above:

$$\|\nabla(u - u_{\mathcal{T}^h})\|_{L^2(\Omega)} \leq c^* \left\{ \sum_{K \in \mathcal{T}^h} h_K^2 \|r\|_{L^2(K)}^2 + \sum_{e \in \mathcal{E}} h_e \|j\|_{L^2(e)}^2 \right\}^{\frac{1}{2}}. \quad (49)$$

The upper bounds are global concerning the domain. The right-hand side of equation can be used as an a posteriori error indicator. To evaluate integrals for equation (49), one should approximate integrals by appropriate quadrature formulas or f and g should be approximated by simpler polynomial functions. Both approaches are often equivalent for generating a posteriori estimators.

Furthermore, one wants to bound the error $\|\nabla(u - u_{\mathcal{T}^h})\|_{L^2(\Omega)}$ from below. The lower bounds are local because the error indicator assigned to an element is bounded by the error on the given element and neighboring elements. To start with, one should replace functions f and g by their mean values

$$f_K = \frac{1}{|K|} \int_K f \text{ and } g_e = \frac{1}{h_e} \int_e g.$$

The next important step for deriving the a posteriori error estimates is introducing the local cut-off functions and inverse estimates for them. One can see definitions and intermediate steps for obtaining a lower bound in [Ver13, Chapter 1]. Let c_* be a constant that only depends on the shape parameter of \mathcal{T}^h and K_e a union of all elements sharing an edge with K . The final results, presented in [Ver13, Theorem 1.5], are a posteriori error indicator

$$\eta_{R,K} = \left\{ h_K^2 \|f_K + \Delta u_{\mathcal{T}^h}\|_{L^2(K)}^2 + \frac{1}{2} \sum_{e \in \mathcal{E}_{K,\Omega}} h_e \|\mathcal{J}_e(\mathbf{n}_e \cdot \nabla u_{\mathcal{T}^h})\|_{L^2(e)}^2 + \sum_{e \in \mathcal{E}_{K,\Gamma_N}} h_e \|g_e - \mathbf{n}_e \cdot \nabla u_{\mathcal{T}^h}\|_{L^2(e)}^2 \right\}^{\frac{1}{2}}, \quad (50)$$

and the estimates

$$\|\nabla(u - u_{\mathcal{T}^h})\|_{L^2(\Omega)} \leq c^* \left\{ \sum_{K \in \mathcal{T}^h} \eta_{R,K}^2 + \sum_{K \in \mathcal{T}^h} h_K^2 \|f - f_K\|_{L^2(K)}^2 + \sum_{e \in \mathcal{E}_{\Gamma_N}} h_e \|g - g_e\|_{L^2(e)}^2 \right\}^{\frac{1}{2}}, \quad (51)$$

and

$$\eta_{R,K} \leq c_* \left\{ \|\nabla(u - u_{\mathcal{T}^h})\|_{L^2(K_e)}^2 + \sum_{K' \subset K_e} h_{K'}^2 \|f - f_{K'}\|_{L^2(K')}^2 + \sum_{e \in \mathcal{E}_{K,\Gamma_N}} h_e \|g - g_e\|_{L^2(e)}^2 \right\}^{\frac{1}{2}}, \quad (52)$$

The upper bound in the estimate (51) shows that in the case when an equation where error indicator $\eta_{R,K}$ is less than tolerance ϵ implies that the true error is also less than the tolerance up to the multiplicative constant c^* . The error indicator is then called reliable. On the other hand, by providing a lower bound in the estimate (52), the error indicator is efficient, i.e., an equation where error indicator $\eta_{R,K}$ is greater than tolerance ϵ implies that the true error is also greater than the tolerance up to the multiplicative constant c_* .

3.4 Ways for refining the mesh

This section shows how to obtain adaptive discretizations using the following processes: refinement, coarsening, and smoothing of meshes. The key ingredient is an a posteriori error indicator. The processes are introduced using the literature [Ver13], [D96], [Ver94], [CM10], [SS05], [BS97] and [Che05].

To start with, the idea of the mesh refinement is the following. Given an error indicator for all $K \in \mathcal{T}^{h_k}$, one needs an algorithm that uses this information to construct the next mesh $\mathcal{T}^{h_{k+1}}$. There are two steps to obtain this task. First, the marking strategy is a problem of selecting elements to be refined. In the second step, the refinement rules determine the construction of a new subdivision. Considering Algorithm 3.1, one wants to make the number of iterations as small as possible since a discrete problem has to be solved in every iteration. Thus, the marking strategy should select sufficiently many mesh elements for refinement in each iteration, but not too many elements than is needed to reduce the error below the prescribed tolerance. Among all marking strategies, it is heuristically assumed that the mesh is optimal when the local error is equally distributed for all elements of the mesh. That means that the local error indicators are equally distributed since the true error is not known. Furthermore, elements that will be marked for refinement are elements with a large local error indicator. On the other hand, elements with a very small local error indicator are unchanged or can be coarsened.

One of the most used marking strategies in adaptive finite element methods is the maximum strategy. Define β as a threshold where $0 < \beta < 1$. Let $\eta_{\max} = \max_{K \in \mathcal{T}^{h_k}} \eta_{R,K}$ and mark K if $\eta_{R,K} \geq \beta \eta_{\max}$. Then, marked K should be placed in a set $\tilde{\mathcal{T}}^{h_k}$, a subset of marked elements that should be refined. When β is close to 0, one refines globally and an unnecessary amount of degrees of freedom is obtained. When β is close to 1 and the error is not equally distributed, one marks a small number of triangles. Thus, to fix this, one should do more iterations, which is costly. Therefore this strategy won't be efficient so β is typically set at the value 0.5. This strategy is cheap and often yields satisfactory results.

Another widely used marking strategy is the equilibrium strategy that is presented with the following algorithm.

Algorithm 3.2. [Ver13, Algorithm 2.2] Given a partition \mathcal{T}^{h_k} , error indicators $\eta_{R,K}$ for the elements $K \in \mathcal{T}^{h_k}$, and a threshold $\beta \in (0,1)$. The goal is to seek for a subset $\tilde{\mathcal{T}}^{h_k}$ of marked elements that should be refined.

(1) Compute $\Theta_{\mathcal{T}^{h_k}} = \sum_{K \in \mathcal{T}^{h_k}} \eta_{R,K}^2$. Set $\sum_{\mathcal{T}^{h_k}} = 0$ and $\tilde{\mathcal{T}}^{h_k} = \emptyset$.

(2) If $\sum_{\mathcal{T}^{h_k}} \geq \beta \Theta_{\mathcal{T}^{h_k}}$ return $\tilde{\mathcal{T}}^{h_k}$; stop. Otherwise go to step (3).

(3) Compute $\tilde{\eta}_{\max} = \max_{K \in \mathcal{T}^{h_k} \setminus \tilde{\mathcal{T}}^{h_k}} \eta_{R,K}$.

(4) For all elements $K \in \mathcal{T}^{h_k} \setminus \tilde{\mathcal{T}}^{h_k}$ check whether $\eta_{R,K} = \tilde{\eta}_{\max}$. If this is the case, put K in $\tilde{\mathcal{T}}^{h_k}$ and add $\eta_{R,K}^2$ to $\sum_{\mathcal{T}^{h_k}}$. Otherwise skip K . When all elements have been checked, return to step (2).

At the end of the algorithm, the set $\tilde{\mathcal{T}}^{h_k}$ satisfies:

$$\sum_{K \in \tilde{\mathcal{T}}^{h_k}} \eta_{R,K}^2 \geq \beta \sum_{K \in \mathcal{T}^{h_k}} \eta_{R,K}^2.$$

A small value of β leads to a small set $\tilde{\mathcal{T}}^{h_k}$ and a large value of β leads to a large set $\tilde{\mathcal{T}}^{h_k}$, i.e., almost all elements are marked.

After the decision which elements should be refined with marking strategies, one has to decide based on the element geometry, how to perform the refinement. The refinement process has two stages. First, one wants to get a subset $\tilde{\mathcal{T}}^{h_k}$ of \mathcal{T}^{h_k} . For that, so-called red-refinement is used (regular refinement). In the second stage, one uses a red-green-blue-refinement of further elements to avoid hanging nodes (irregular refinement). Hanging nodes are vertices where the triangulation condition that two triangles share at most a common edge or a common vertex is violated.

Given $K \in \mathcal{T}^{h_k}$ and edges E_1, E_2, E_3 of K where E_1 is the longest edge, a red-refinement of K is derived by dividing K into four new sub-triangles. That is obtained by joining the midpoints of its edges. They are similar to the parent element, thus they have the same angles and the shape parameter of the elements doesn't change. A blue-refinement of K is derived by dividing K into three sub-triangles by joining the midpoint of E_1 with the opposite vertex and the midpoint of E_2 or E_3 . A green-refinement of K is derived by dividing K into two sub-triangles by joining the midpoint of the longest edge E_1 with the opposite vertex. The refinements are illustrated in Figure 1.

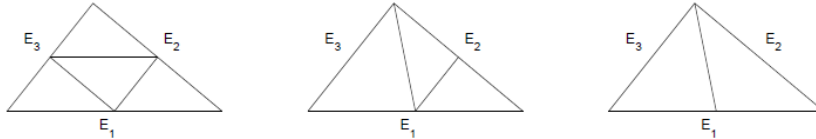


Figure 1: Red, blue and green refinement [CM10, Figure 6.1.]

Too acute or too obtuse triangles and hanging nodes are avoided using the following rules [Ver94].

(1) A triangle having three hanging nodes uses red-refinement.

(2) A triangle having two hanging nodes uses blue-refinement, if one of them lies on the longest edge of the triangle; otherwise it uses red-refinement.

(3) A triangle having one hanging node uses green-refinement, if the hanging node lies on its longest edge; otherwise uses blue-refinement.

The rules (2) and (3) can lead to new hanging nodes.

An alternative strategy to the red-refinement is the marked-edge bisection. Then one bisects triangles only by dividing a marked edge. The following rules for it are established. The coarsest mesh is formed in a way that the longest edge of any element is also the longest edge of the adjacent element except if it is a boundary edge. Only the longest edge of every element in the coarsest mesh is marked. The element is bisected by connecting the midpoint of its marked edge with the opposite vertex. Then, its two unmarked edges are marked edges of the two new triangles. Figure 2 shows the process, where marked edges are labeled with \bullet .

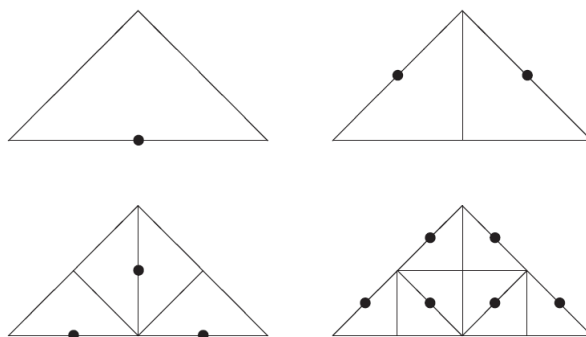


Figure 2: Marked edge bisection [Ver13, Figure 2.5.]

The next used technique is the mesh coarsening. It is the inverse process of refinement. As in the refinement process, the main goal for coarsening is to equally distribute the local errors. The idea for the coarsening process is to gather all elements that were created during the refinement such that their parents build a corresponding refinement patch. After the coarsening process, refinement edges are back at their original position on parent elements. Furthermore, an element will be coarsened if all involved neighbor elements are marked for coarsening. In contrast, during refinement, it is possible that by bisecting an element, an unmarked element is also refined in order to keep the mesh conforming. Therefore, in the adaptive method, this assures that if the local error indicator is not small enough no element is coarsened. On the other hand, marked elements with a large local error indicator are refined. One should remark that after the coarsening process, the local error should not be larger than the tolerance used for refinement. If it is, then in the next iteration the elements would be refined again and the desired results might never be obtained. The negative aspect of coarsening is that additional errors can be produced and some information can be lost during the process. The suggestion to avoid the loss of information is to delay the mesh coarsening until the final iteration of the adaptive procedure. Furthermore, one can use the marking strategies defined above to mark mesh elements for coarsening. The following algorithm is a modification of the maximum strategy defined for element's marking and it is best suited for the marked edge bisection.

Let \mathcal{T}^{h_k} be a current partition, K an element of it and $n \in \mathcal{N}$ a vertex of it. K has refinement level l if it is obtained by subdividing an element of the coarsest partition l times. If there exists a vertex of K which is not a vertex of its parent triangle K' , then it is called the refinement vertex of K . Finally, a vertex $n \in \mathcal{N}$ and patch K_n are resolvable if n is the refinement vertex of all elements in K_n and if all elements in K_n have the same refinement level.

Algorithm 3.3. [Ver13, Algorithm 2.4] *Given a partition \mathcal{T}^{h_k} , error indicators $\eta_{R,K}$ for all elements $K \in \mathcal{T}^{h_k}$, and parameters $0 < \beta_1 < \beta_2 < 1$. The goal is to find subsets \mathcal{T}_c and \mathcal{T}_r of elements that should be coarsened and refined, respectively.*

(1) Set $\mathcal{T}_c = \emptyset$, $\mathcal{T}_r = \emptyset$ and compute $\eta_{\max} = \max_{K \in \mathcal{T}^{h_k}} \eta_{R,K}$

(2) For all $K \in \mathcal{T}^{h_k}$ check whether $\eta_{R,K} \geq \beta_2 \eta_{\max}$. If this is the case, put K in \mathcal{T}_r .

(3) For all vertices $n \in \mathcal{N}$ check whether n is resolvable. If this is the case and if $\max_{K \subset K_n} \eta_{R,K} \leq \beta_1 \eta_{\max}$, put all elements contained in K_n into \mathcal{T}_c .

One can notice that this algorithm simultaneously refines and coarsen elements of the current partition and in that way, it constructs the partition of the next level.

The next technique is the mesh smoothing. This method doesn't change the topology in the triangulation as the above two methods do and that is the critical ability to the success of an adaptive method. Therefore, a mesh smoothing algorithm cannot be the basis of an effective adaptive method. Instead, it complements mesh-refinement methods. After creating a mesh with mesh-refinement methods where a proper density of mesh vertices and topology is obtained, one uses a smoothing algorithm to improve the quality of a mesh. That means that the vertices move a little but the number of elements and the adjacency stay unchanged. The result of a vertex movement is error reduction. Even small movements of the vertices can result in a high error reduction. This method can be used when further refinement is impossible. In this section, the focus is on triangular meshes, i.e., all partitions consist of triangles.

The mesh-smoothing algorithms follow a strategy similar to Gauss-Seidel which optimizes a quality function q . A quality function q assigns a non-negative number to every element. One can see the different choices for q and their properties in [BS97]. A larger value of q shows a better quality. Given a triangulation \mathcal{T}^{h_k} one wants to obtain a new improved triangulation $\tilde{\mathcal{T}}^{h_k}$ with the same topology as \mathcal{T}^{h_k} such that the error is minimized. One seeks the solution of the optimization problem

$$\min_{\tilde{K} \in \tilde{\mathcal{T}}^{h_k}} q(\tilde{K}) > \min_{K \in \mathcal{T}^{h_k}} q(K).$$

Therefore, several iterations of a strategy similar to Gauss-Seidel should be performed. There one should go through the vertices and locally optimize the position of a single vertex while having all others fixed. In other words, for every vertex $n \in \mathcal{T}^{h_k}$, fix the vertices of the boundary of K_n and find a new vertex \tilde{n} inside K_n such that

$$\min_{\tilde{K} \subset K_{\tilde{n}}} q(\tilde{K}) > \min_{K \subset K_n} q(K).$$

This is the local optimization problem and its solution depends on the choice of the quality function q .

Now that techniques for refining the mesh are introduced, the following example from [Ver13, Page 3] and [Che05, Example 6.1.] is presented to show the potential of the adaptive refinement method. The domain Ω is defined as a circular segment with radius one, angle $\frac{3}{2}\pi$ and center at the origin. The problem (22)-(24) is considered on Ω . Thus, a function u is harmonic in the interior of Ω , it vanishes on the straight parts of the boundary $\partial\Omega$ and it has a normal derivative $\frac{2}{3}\sin(\frac{2}{3}\gamma)$ on the curved part of the boundary. In terms of polar coordinates, one gets that the exact solution is $u = r^{\frac{2}{3}}\sin(\frac{2}{3}\gamma)$. Furthermore, one calculates the Ritz projections $u_{\mathcal{T}^h}$ of u onto the spaces of continuous piecewise linear finite elements. Those spaces are associated with the two triangulations shown in Figure 3.

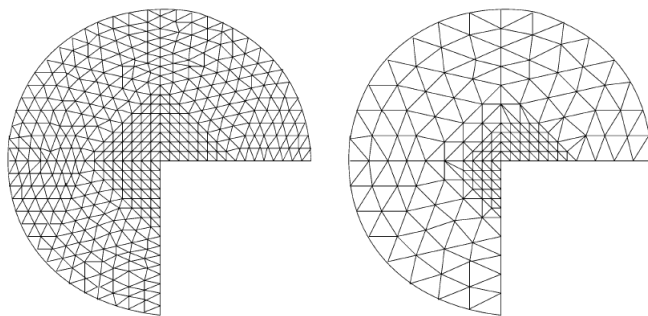


Figure 3: Uniform and adaptive triangulations [Che05, Figure 6.8.]

The left triangulation represents the triangulation obtained by uniform refinement and the right one is obtained by an adaptive refinement of meshes. The right triangulation is constructed from an initial triangulation \mathcal{T}^{h_0} by using Algorithm 3.1. based on the error estimator $\eta_{R,K}$. Specifically, the adaptive refinement strategy of Algorithm 3.1 is used. A triangle $K \in \mathcal{T}^{h_k}$ is refined if $\eta_{R,K} \geq 0.5 \max_{K' \in \mathcal{T}^{h_k}} \eta_{R,K'}$. The right triangulation in Figure 3 is obtained such that a triangle $K \in \mathcal{T}^{h_k}$ is divided into four smaller triangles by connecting the midpoints of its edges if $\eta_{R,K} \geq 0.5 \max_{K' \in \mathcal{T}^{h_k}} \eta_{R,K'}$. The midpoint of an edge having its two endpoints on $\partial\Omega$ is projected onto $\partial\Omega$. The left triangulation is also constructed from initial triangulation \mathcal{T}^{h_0} which is composed of three right-angled isosceles triangles with short edges of unit length. The left triangulation in Figure 3 is obtained by five uniform refinements of \mathcal{T}^{h_0} . In each refinement step, as described above, every triangle $K \in \mathcal{T}^{h_k}$ is divided into four smaller triangles by connecting the midpoints of its edges. Again, the midpoint of an edge having its two endpoints on $\partial\Omega$ is projected onto $\partial\Omega$. For the final result, there are 3072 triangles and 1552 unknowns in uniform refinement, while there are 298 triangles and 143 unknowns in adaptive refinement. Also, the relative error $\frac{\|\nabla(u - u_{\mathcal{T}^h})\|_{L^2(\Omega)}}{\|\nabla u\|_{L^2(\Omega)}}$ is lower with adaptive refinement. Therefore, one can see the advantages of the adaptive refinement strategy.

4 Convergence of an adaptive algorithm

This section presents the proof of the convergence of the adaptive Algorithm 3.1 following the proof from [Ver13, Chapter 1.14]. Further used literature is [MNS02], [D96] and [Beb03].

One considers the problem (22)-(24) with homogeneous Neumann boundary Γ_N , thus (24) is defined as $n \cdot \nabla u = 0$ on Γ_N . As mentioned before, Algorithm 3.1 uses the residual error indicator $\eta_{R,K}$, and a suitable marking strategy in step (4). After providing all the necessary data, the goal is to prove that an algorithm gives a sequence of discrete solutions that converge to the true solution of the differential equation. Also, some remarks on refinement strategies are made, as well as how to apply them to obtain the results.

The idea is to show convergence when the right-hand side is general and not restricted as piecewise constant. To start with, the procedure for a piecewise constant right-hand side is presented, therefore, assume that f is piecewise constant on all partitions. Let \mathcal{T}^{h_1} be a triangulation of Ω , and define its subset $\tilde{\mathcal{T}}^{h_1}$ in the marking strategy of Algorithm 3.2. Let \mathcal{T}^{h_2} be a refinement of \mathcal{T}^{h_1} satisfying $S_D^{1,0}(\mathcal{T}^{h_1}) \subset S_D^{1,0}(\mathcal{T}^{h_2})$, i.e, the finite element spaces are nested. This property is crucial for error reduction and a sequence of nested spaces can be obtained by using refinement by bisection. Assume that

$$\text{each element of } \tilde{\mathcal{T}}^{h_1}, \text{ and also each of its faces, contains a node of } \mathcal{T}^{h_2} \text{ in its interior.} \quad (53)$$

In particular, for every 1-face, i.e., edge, this condition can be interpreted in a way that the midpoint of every edge of every element in $\tilde{\mathcal{T}}^{h_1}$ is a node of an element in \mathcal{T}^{h_2} . One can fulfill the special refinement (53) by applying either two steps of the red-refinement, or three steps of the marked edge bisection to every element in $\tilde{\mathcal{T}}^{h_1}$. Define by u_1 and u_2 the unique solutions of problem (29) that correspond to the partitions \mathcal{T}^{h_1} and \mathcal{T}^{h_2} , respectively. The goal is to show that there exists a constant $0 < \alpha < 1$ such that

$$\|\nabla(u - u_2)\|_{L^2(\Omega)}^2 \leq \alpha^2 \|\nabla(u - u_1)\|_{L^2(\Omega)}^2.$$

This means that by every iteration of Algorithm 3.1, the error is reduced at least by the factor α . Then Algorithm 3.1 converges when f is piecewise constant on the coarsest partition \mathcal{T}^{h_0} . To obtain α some estimates and inequalities should be presented.

Lemma 4.1. [MNS02, Lemma 4.1] If \mathcal{T}^{h_2} is a local refinement of \mathcal{T}^{h_1} , such that $S_D^{1,0}(\mathcal{T}^{h_1}) \subset S_D^{1,0}(\mathcal{T}^{h_2})$, the following relation holds:

$$\|\nabla(u - u_2)\|_{L^2(\Omega)}^2 = \|\nabla(u - u_1)\|_{L^2(\Omega)}^2 - \|\nabla(u_1 - u_2)\|_{L^2(\Omega)}^2. \quad (54)$$

Proof. By Galerkin orthogonality, $u_2 - u_1$ is perpendicular to $u - u_2$. Therefore, since $u - u_1 = (u - u_2) + (u_2 - u_1)$, (54) follows from the Pythagoras theorem. \square

As mentioned in the last section, using Algorithm 3.2 to obtain $\tilde{\mathcal{T}}^{h_1}$ of \mathcal{T}^{h_1} , where $\beta \in (0, 1)$, one gets that $\tilde{\mathcal{T}}^{h_1}$ satisfies

$$\sum_{K \in \tilde{\mathcal{T}}^{h_1}} \eta_{R,K}^2 \geq \beta \sum_{K \in \mathcal{T}^{h_1}} \eta_{R,K}^2. \quad (55)$$

The terms $h_K \|f - f_K\|_{L^2(K)}$ and $h_e^{\frac{1}{2}} \|g - g_e\|_{L^2(e)}$ in equation (51) are called data oscillations. Since f is piecewise constant on \mathcal{T}^{h_1} , the term $h_K \|f - f_K\|_{L^2(K)}$ vanishes. The term $h_e^{\frac{1}{2}} \|g - g_e\|_{L^2(e)}$ vanishes because the Neumann boundary condition is homogeneous. Therefore, equation (51) implies

$$\|\nabla(u - u_1)\|_{L^2(\Omega)}^2 \leq c^{*2} \sum_{K \in \mathcal{T}^{h_1}} \eta_{R,K}^2. \quad (56)$$

Using estimates (55) and (56), one can conclude that

$$\|\nabla(u - u_1)\|_{L^2(\Omega)}^2 \leq \frac{c^{*2}}{\beta} \sum_{K \in \tilde{\mathcal{T}}^{h_1}} \eta_{R,K}^2. \quad (57)$$

The special refinement (53) is required to obtain further results. One can find intermediate steps in [Ver13, Chapter 1]. The final estimate is

$$\sum_{K \in \tilde{\mathcal{T}}^{h_1}} \eta_{R,K}^2 \leq c_*^2 \|\nabla(u_2 - u_1)\|_{L^2(\Omega)}^2. \quad (58)$$

Furthermore, estimates (57) and (58) imply

$$-\|\nabla(u_2 - u_1)\|_{L^2(\Omega)}^2 \leq -\frac{1}{c_*^2} \sum_{K \in \tilde{\mathcal{T}}^{h_1}} \eta_{R,K}^2 \leq -\frac{\beta}{c_*^2 c^{*2}} \|\nabla(u - u_1)\|_{L^2(\Omega)}^2. \quad (59)$$

Using the estimates (54) and (59), one obtains that

$$\begin{aligned} \|\nabla(u - u_2)\|_{L^2(\Omega)}^2 &= \|\nabla(u - u_1)\|_{L^2(\Omega)}^2 - \|\nabla(u_1 - u_2)\|_{L^2(\Omega)}^2 \\ &\leq \left(1 - \frac{\beta}{c_*^2 c^{*2}}\right) \|\nabla(u - u_1)\|_{L^2(\Omega)}^2. \end{aligned}$$

Thus, α is defined as $\alpha = \sqrt{1 - \frac{\beta}{c_*^2 c^{*2}}}$, and the above-mentioned statement implies that Algorithm 3.1 converges when f is piecewise constant. Also, one should remark that α depends on the parameter β and the shape parameter of \mathcal{T}^{h_0} .

The procedure for the general right-hand side is presented in the following, thus let $f \in L^2(\Omega)$ be an arbitrary function. An approximation by piecewise constants is required for resolving the right-hand side. Given an arbitrary partition \mathcal{T}^h , let $f_{\mathcal{T}^h}$ be the L^2 -projection of f onto the space of piecewise constant functions corresponding to \mathcal{T}^h . It is defined as $f_{\mathcal{T}^h} = \sum_{K \in \mathcal{T}^h} f_K \chi_K$, where χ_K denotes the characteristic function of the set K . $f_{\mathcal{T}^h}$ is the $L^2(\Omega)$ best approximation to f by piecewise constants dependent on \mathcal{T}^h . Let u and \tilde{u} denote the unique solutions of problem (26) with right-hand sides f and $f_{\mathcal{T}^h}$, respectively. Denote by $u_{\mathcal{T}^h}$ and $\tilde{u}_{\mathcal{T}^h}$ the unique solutions of the discrete problem (29) with right-hand sides f and $f_{\mathcal{T}^h}$, respectively. $u_{\mathcal{T}^h}$ is the best approximation to u in $S_D^{1,0}(\mathcal{T}^h)$ with respect to the norm $\|\nabla \cdot\|_{L^2(\Omega)}$, thus one has

$$\|\nabla(u - u_{\mathcal{T}^h})\|_{L^2(\Omega)} \leq \|\nabla(u - \tilde{u}_{\mathcal{T}^h})\|_{L^2(\Omega)}. \quad (60)$$

Applying the triangle inequality on the right-hand side of the inequality (60) implies

$$\|\nabla(u - \tilde{u}_{\mathcal{T}^h})\|_{L^2(\Omega)} \leq \|\nabla(u - \tilde{u})\|_{L^2(\Omega)} + \|\nabla(\tilde{u} - \tilde{u}_{\mathcal{T}^h})\|_{L^2(\Omega)}.$$

Therefore, it holds

$$\|\nabla(u - u_{\mathcal{T}^h})\|_{L^2(\Omega)} \leq \|\nabla(u - \tilde{u})\|_{L^2(\Omega)} + \|\nabla(\tilde{u} - \tilde{u}_{\mathcal{T}^h})\|_{L^2(\Omega)}. \quad (61)$$

For the term $\|\nabla(\tilde{u} - \tilde{u}_{\mathcal{T}^h})\|_{L^2(\Omega)}$ one can apply the procedure for the piecewise constant right-hand sides shown before. For the term $\|\nabla(u - \tilde{u})\|_{L^2(\Omega)}$, one wants to show again, that every iteration of the modified Algorithm 3.1 reduces $\|\nabla(u - \tilde{u})\|_{L^2(\Omega)}$ by some factor. Through this section, it is shown that in order to control the term $\|\nabla(u - \tilde{u})\|_{L^2(\Omega)}$ one should control data oscillation. To connect this term with $h_K \|f - f_K\|_{L^2(K)}$, one should first define $v = u - \tilde{u}$ and apply it into equation (40). Therefore, one obtains

$$\|\nabla(u - \tilde{u})\|_{L^2(\Omega)} = \sup_{w \in H_D^1(\Omega) \setminus \{0\}} \frac{1}{\|\nabla w\|_{L^2(\Omega)}} \int_{\Omega} \nabla(u - \tilde{u}) \cdot \nabla w.$$

Since u and \tilde{u} are solutions to the problem (26) with right-hand sides f and $f_{\mathcal{T}^h}$, respectively, one gets that for every $w \in H_D^1(\Omega)$,

$$\int_{\Omega} \nabla(u - \tilde{u}) \cdot \nabla w = \int_{\Omega} (f - f_{\mathcal{T}^h}) w.$$

Let w_K be defined as the integral mean value of w over K . Because of the definition of $f_{\mathcal{T}^h}$ as L^2 -projection one can conclude that

$$\int_{\Omega} (f - f_{\mathcal{T}^h}) w = \int_{\Omega} (f - f_{\mathcal{T}^h})(w - w_{\mathcal{T}^h}) = \sum_{K \in \mathcal{T}^h} \int_K (f - f_K)(w - w_K).$$

Therefore, combining previous equalities, it is obtained

$$\int_{\Omega} \nabla(u - \tilde{u}) \cdot \nabla w = \sum_{K \in \mathcal{T}^h} \int_K (f - f_K)(w - w_K).$$

Now, using the Cauchy–Schwarz inequality on each of the terms in the last sum, it follows

$$\int_{\Omega} \nabla(u - \tilde{u}) \cdot \nabla w \leq \sum_{K \in \mathcal{T}^h} \|f - f_K\|_{L^2(K)} \|w - w_K\|_{L^2(K)}.$$

The modification of the classical Poincaré inequality, Theorem A.4, will be used for the next step. It is practical to know an explicit expression for the constant C_p in (18). In the case of convex domains, this constant is $\frac{d}{\pi}$, where d is the diameter of Ω . Here, every element K is convex and h_K is the diameter of K . One can check more details in [Ver13, Chapter 3], and conclude that for all elements it holds

$$\|w - w_K\|_{L^2(K)} \leq \frac{h_K}{\pi} \|\nabla w\|_{L^2(K)}.$$

Then by combining the previous expressions, bounding the last terms with the modified Poincaré inequality, and applying a weighted Cauchy–Schwarz inequality, one gets

$$\|\nabla(u - \tilde{u})\|_{L^2(\Omega)} \leq \frac{1}{\pi} \left\{ \sum_{K \in \mathcal{T}^h} h_K^2 \|f - f_K\|_{L^2(K)}^2 \right\}^{\frac{1}{2}}.$$

Therefore, in the case of general right-hand sides f , the right-hand side of this estimate, i.e., data oscillation, should be controlled. To obtain that, one should change Algorithms 3.1 and 3.2. First, in Algorithm 3.2, $\eta_{R,K}^2$ is replaced with $h_K^2 \|f - f_K\|_{L^2(K)}^2$. Let \mathcal{T}^{h_1} , \mathcal{T}^{h_2} , $\tilde{\mathcal{T}}^{h_1}$ be defined as in the beginning of the section and let $\beta \in (0, 1)$. With the changed Algorithm 3.2, a subset $\tilde{\mathcal{T}}^{h_1}$ of \mathcal{T}^{h_1} satisfies

$$\sum_{K \in \tilde{\mathcal{T}}^{h_1}} h_K^2 \|f - f_K\|_{L^2(K)}^2 \geq \beta \sum_{K \in \mathcal{T}^{h_1}} h_K^2 \|f - f_K\|_{L^2(K)}^2.$$

Assume that

every element $K \in \tilde{\mathcal{T}}^{h_1}$ is the union of elements $\hat{K} \in \mathcal{T}^{h_2}$ such that

$$h_{\hat{K}} \leq \frac{1}{2} h_K.$$

One can obtain this special condition by applying to every element in $\tilde{\mathcal{T}}^{h_1}$ either two steps of the red refinement or three steps of the marked edge bisection. The set \mathcal{T}^{h_2} can be split into two disjoint subsets \mathcal{T}^{h_B} and \mathcal{T}^{h_A} such that $\bigcup_{\hat{K} \in \mathcal{T}^{h_2}} \hat{K} = \bigcup_{K \in \tilde{\mathcal{T}}^{h_1}} K$. One has:

$$\begin{aligned} \sum_{K \in \mathcal{T}^{h_2}} h_K^2 \|f - f_K\|_{L^2(K)}^2 &= \sum_{\hat{K} \in \mathcal{T}^{h_A}} h_{\hat{K}}^2 \|f - f_{\hat{K}}\|_{L^2(\hat{K})}^2 + \sum_{K \in \mathcal{T}^{h_B}} h_K^2 \|f - f_K\|_{L^2(K)}^2 \\ &\leq \frac{1}{4} \sum_{K \in \tilde{\mathcal{T}}^{h_1}} h_K^2 \|f - f_K\|_{L^2(K)}^2 + \sum_{\substack{K \in \\ \mathcal{T}^{h_1} \setminus \tilde{\mathcal{T}}^{h_1}}} h_K^2 \|f - f_K\|_{L^2(K)}^2 \\ &= \frac{1}{4} \sum_{K \in \tilde{\mathcal{T}}^{h_1}} h_K^2 \|f - f_K\|_{L^2(K)}^2 + \sum_{K \in \mathcal{T}^{h_1}} h_K^2 \|f - f_K\|_{L^2(K)}^2 \\ &\quad - \sum_{K \in \tilde{\mathcal{T}}^{h_1}} h_K^2 \|f - f_K\|_{L^2(K)}^2 \\ &= \sum_{K \in \mathcal{T}^{h_1}} h_K^2 \|f - f_K\|_{L^2(K)}^2 - \frac{3}{4} \sum_{K \in \tilde{\mathcal{T}}^{h_1}} h_K^2 \|f - f_K\|_{L^2(K)}^2 \\ &\leq \left(1 - \frac{3\beta}{4}\right) \sum_{K \in \mathcal{T}^{h_1}} h_K^2 \|f - f_K\|_{L^2(K)}^2. \end{aligned}$$

Furthermore, Algorithm 3.1 should be changed. To do this, step (2) is left out and in step (3), the a posteriori error estimate is replaced by $h_K \|f - f_K\|_{L^2(K)}$. Thus, by every iteration, $\|\nabla(u - \tilde{u})\|_{L^2(\Omega)}$ is reduced at least by the factor $\sqrt{1 - \frac{3\beta}{4}}$.

To conclude, given a partition \mathcal{T}^h and any fixed tolerance ϵ , this algorithm provides $\|\nabla(u - \tilde{u})\|_{L^2(\Omega)} \leq \frac{\epsilon}{2}$ after finitely many iterations. Using the adaptive algorithm described at the beginning of this section with partition \mathcal{T}^h as a starting point, after finitely many iterations, one obtains a refined partition $\mathcal{T}^{h'}$ with $\|\nabla(\tilde{u} - \tilde{u}_{\mathcal{T}^{h'}})\|_{L^2(\Omega)} \leq \frac{\epsilon}{2}$. From (61) one can conclude that $\|\nabla(u - u_{\mathcal{T}^{h'}})\|_{L^2(\Omega)} \leq \epsilon$.

5 Numerical Studies

This section presents the results of simulations of two numerical examples. Both examples inspect the Poisson equation (22). In example 5.1, a known solution with a boundary layer is studied. In example 5.2, a known solution with a circular internal layer is studied. The goal is to show the convergence of the adaptive Algorithm 3.1, defined in chapter 3. The used literature is [ABR17], [Joh00], [JS08], [JM04], [JMT97] and [WBA⁺17]. All simulations were performed with the program package ParMooN (Parallel Mathematics and object-oriented Numerics) [WBA⁺17], used for the numerical solution of elliptic and parabolic partial differential equations. It is a modernized version of its predecessor MooNMD [JM04]. The program flow shown in Figure 4 is utilized.

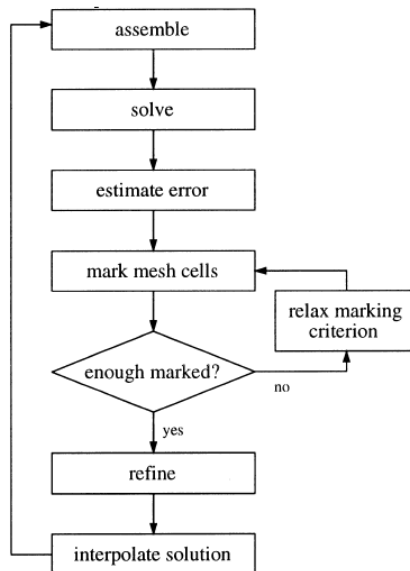


Figure 4: The program flow [Joh00, Figure 1.]

The computation starts on an initial grid, i.e., level 0. The uniform grid refinement is applied until the appropriate level is reached, then the adaptive grid refinement starts. This level has to be found by numerical tests. In the examples presented here, the value of *refinement_max_n_uniform_steps* is set to 2. Then the adaptive refinement iterations are run. It was sufficient to run 20 iterations (*refinement_max_n_adaptive_steps*) in each example to get enough data for the evaluation of results. An error estimator is the next thing that one has to choose. In this case, it is the residual error estimator which is introduced in section 3.3. After its computation, every mesh cell K has a number $\eta_{R,K}$. As mentioned before, these numbers influence which mesh cells should be refined or coarsened. The coarsening process is not important for the stationary problems. The maximum strategy is used as a marking strategy and one can see more details in section 3.4. Let η_{\max} be a reference value which is previously defined as $\eta_{\max} = \max_{K \in \mathcal{T}^h} \eta_{R,K}$ and let $\beta \in (0, 1)$ be a threshold. Then, a mesh cell K will be refined if $\eta_{R,K} \geq \beta \eta_{\max}$. In the examples run

here, this value is set as $\beta = 0.5$. After every adaptive refinement step, a sufficient increase in the number of degrees of freedom should occur. In this way, the expensive assembling and solving a discrete system with only a few new degrees of freedom is prevented. In Figure 4 one can see that during the program flow, the marking criterion is relaxed to allow more mesh cells to be marked for refinement. To obtain that, a minimal amount of mesh cells that have to be marked for refinement per iteration is set. This value is defined as min_ref and in the examples here is set as $min_ref = 0.1 (= 10\%)$. In the case when not sufficiently many mesh cells are marked, β is set as $\beta = \beta/1.1$ and the mesh cells are marked again. Usually, the value of β has to decrease several times before a sufficient number of cells are marked for refinement.

Example 5.1. [ABR17, Example 6.1] (*A known two dimensional solution with a boundary layer*) Let $\epsilon = 10^{-3}$, $\Omega = (0, 1)^2$, and Dirichlet boundary conditions and the right-hand side f such that the exact solution of (22) is given by

$$u(x, y) = y(1 - y) \left(x - \frac{e^{-\frac{(1-x)}{\epsilon}} - e^{-\frac{1}{\epsilon}}}{1 - e^{-\frac{1}{\epsilon}}} \right).$$

A numerical solution is presented in Figure 5.a).

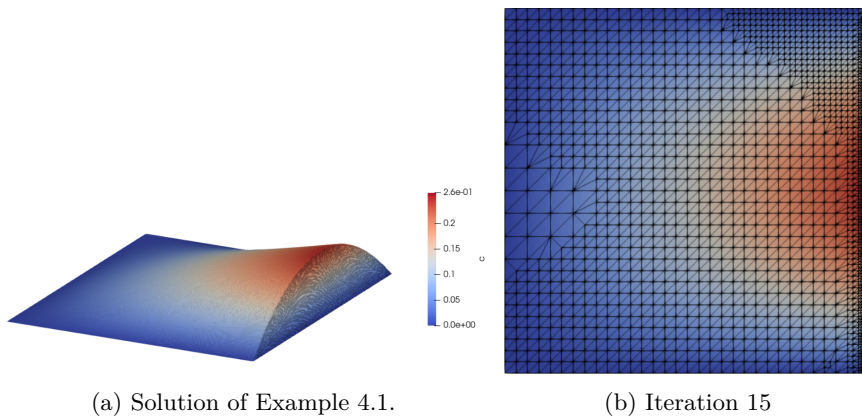


Figure 5: A known two dimensional solution with a boundary layer

Level	Mesh cells	Min mesh cells	Marked mesh cells
0	32	3	4
1	57	5	6
4	361	36	42
10	14771	1477	5377
15	425262	42526	92566

Table 1: Table with information to the number of mesh cells

The development of the mesh through iterations of the Algorithm 3.1 is shown in Figure 6: the top-left (a) is the initial triangulation, top-right (b) is iteration 1, bottom-left (c) is iteration 4 and bottom-right (d) is iteration 10. In

addition, Figure 5.b) presents iteration 15. One can see that the refinement process is concentrated around the boundary layer and the approximate solutions are nonnegative, as well as the true solution. One can find refinement results of the mentioned iterations 0, 1, 4, 10 and 15 in Table 1. In the second column the number of mesh cells is shown. In the third column the minimal amount of mesh cells that have to change is shown. The program also provides the number of cells which are marked for refinement, and that is presented in the fourth column. Therefore, the above-mentioned threshold of required 10% of mesh cells as a minimal amount of mesh cells that must be marked for refinement, is satisfied.

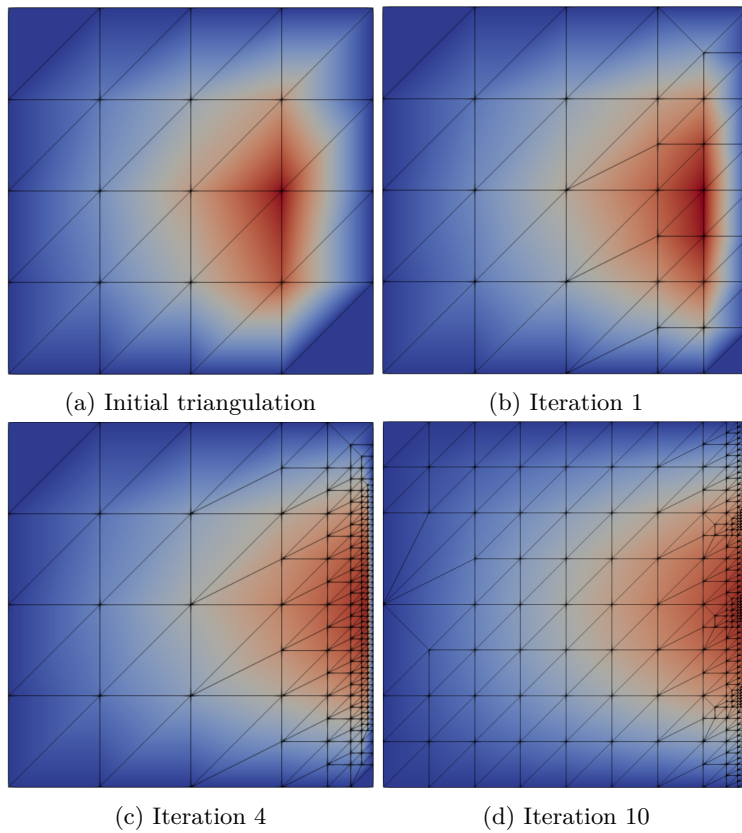


Figure 6: Development of adaptive meshes through iterations of Algorithm 2.1.

Furthermore, the value of η_{\max} decreases with every iteration. As an example, for iteration 0, the value is $\eta_{\max} = 414.405$ while for iteration 17 it is $\eta_{\max} = 0.0006$. Therefore, the value of $\eta_{R,K}$ also decreases. One can see values of η_{\max} per iteration in Figure 7.

Figure 8 shows the increasing number of degrees of freedom, while the error $\|\nabla(u - u_h)\|_{L^2(\Omega)}$ decreases. These results are obtained after 20 iterations. One can see that the error increases until iteration 2 and then it starts to decrease. Once when the mesh is sufficiently refined, the error decreases with the optimal rate. Therefore, the adaptive Algorithm 3.1 converges. With respect to the number of degrees of freedom, the order of convergence is the first order.

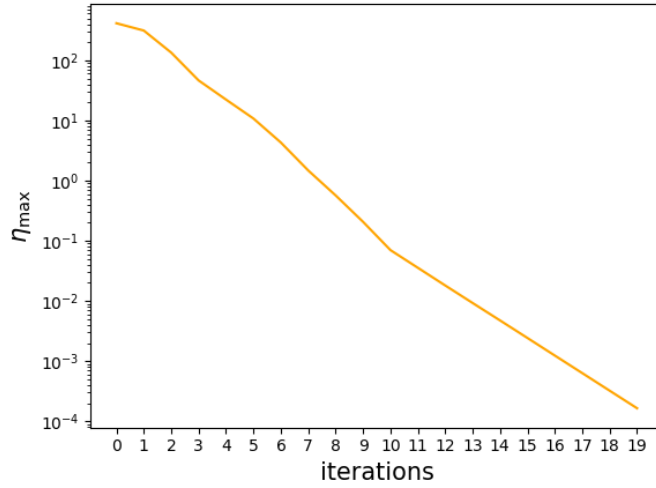


Figure 7: Decreasing values of η_{\max} through iterations

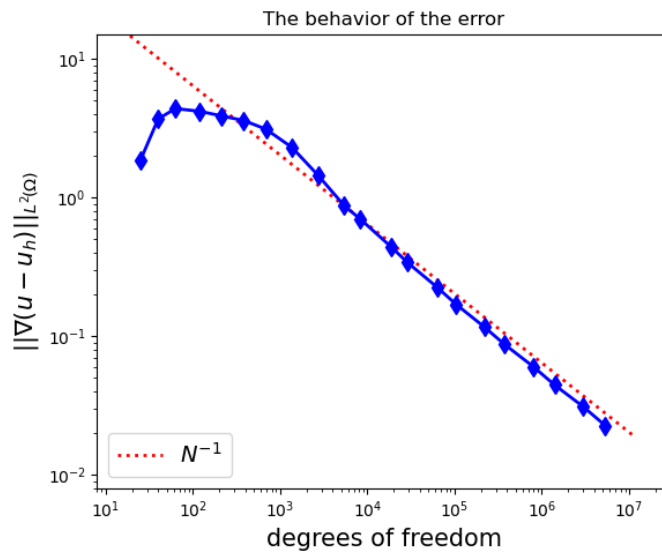


Figure 8: The behavior of the error $\|\nabla(u - u_h)\|_{L^2(\Omega)}$ for adaptive refinement

Figure 9 shows the error of the function in the L^2 -norm using the data of 20 iterations. In the log-log plot, the optimal decrease of $\|u - u_h\|_{L^2(\Omega)}$ is represented with a red dotted line with factor -2 . One can see, that the error decreases optimally as the number of degrees of freedom increases. Thus, it can be concluded, that it is a second order convergence with respect to the L^2 norm of the error.

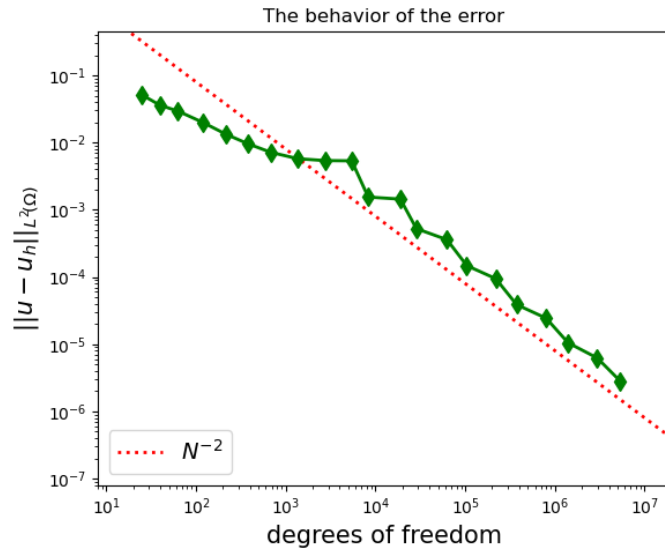


Figure 9: The behavior of the error $\|u - u_h\|_{L^2(\Omega)}$ with respect to the number of degrees of freedom

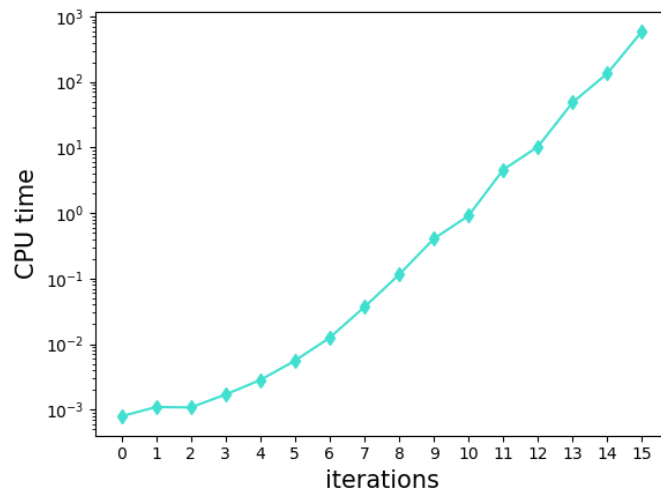


Figure 10: CPU time in seconds through 15 iterations

Furthermore, the number of degrees of freedom increases with every iteration along with the computation time, especially when the number of degrees of freedom is more than 10^5 . As an example, the iteration 1 was executed in 0.001 seconds while the iteration 15 needed 593.837 seconds to be executed. One can see the increasing values of CPU time in Figure 10.

Example 5.2. [JS08, Example 7.2] (*Circular internal layer*) In this example, the right-hand side is chosen such that the solution of the Poisson problem (22) is

$$u(x, y) = 16 \sin(\pi)x(1-x)y(1-y) \times \left(\frac{1}{2} + \frac{\arctan[2\epsilon^{-\frac{1}{2}}(0.25^2 - (x-0.5)^2 - (y-0.5)^2)]}{\pi} \right),$$

with $\epsilon = 10^{-3}$. The problem is considered in $\Omega = (0, 1)^2$. A numerical solution is presented in Figure 11. One can see that it is a hump. The parameter ϵ controls the steepness of the circular internal layer, while $\sqrt{\epsilon}$ represents the thickness of the layer.

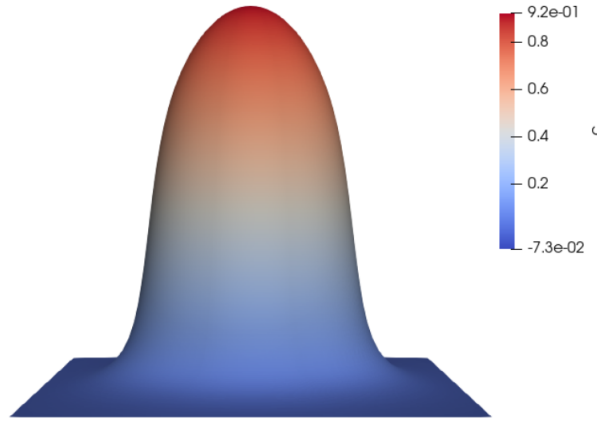


Figure 11: Solution of the example 4.2

Simulations are performed on the adaptively refined grids starting with the same initial grid as in the previous example. Therefore, Figure 12 shows an initial grid with 32 mesh cells.

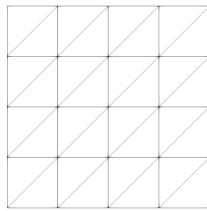


Figure 12: Initial grid

When Algorithm 3.1 with parameters $\beta = 0.5$ and $min.ref = 0.1$ of the maximum marking strategy is applied to the problem, a sequence of grids through iterations is obtained and it is shown in Figure 13. Iteration 1 in 13.(a) has 64 mesh cells, iteration 4 in 13.(b) has 668 cells, iteration 7 in 13.(c) has 7052 cells and iteration 10 in 13.(d) has 52448 cells.

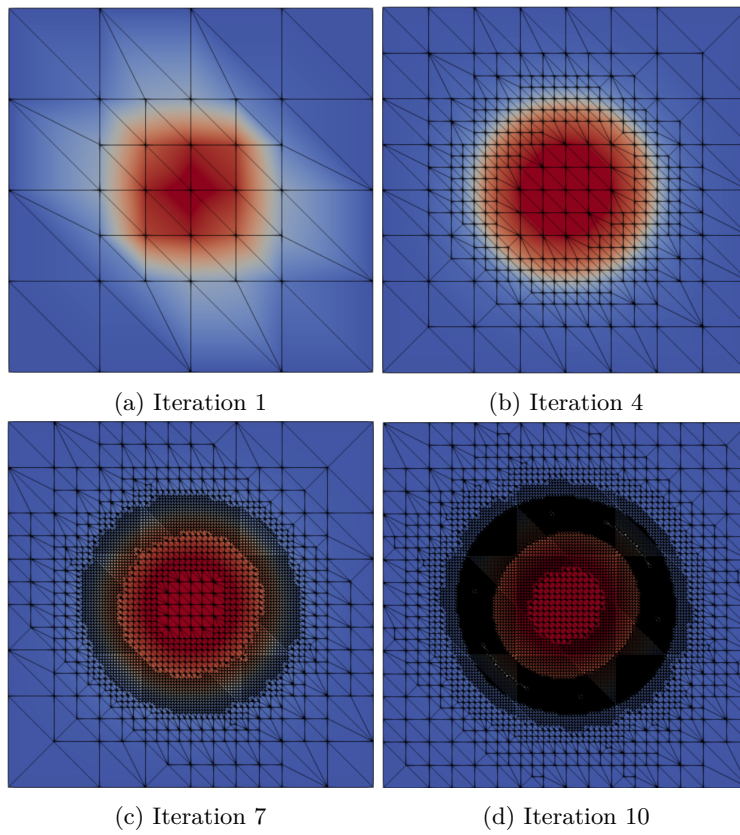


Figure 13: Adaptive refinement of meshes

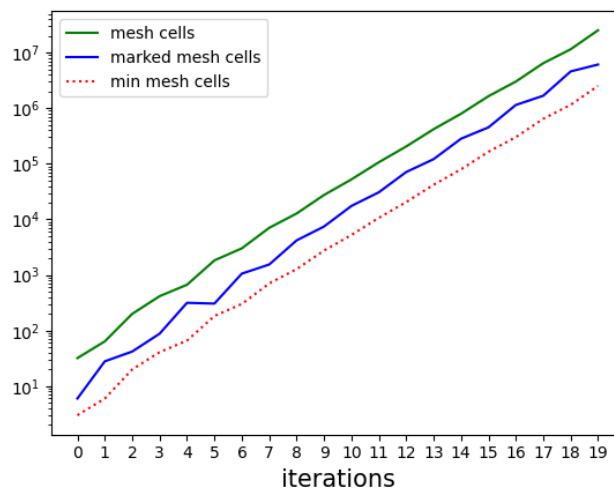


Figure 14: Increasing number of mesh cells through iterations

In Figure 14 one can see the number of mesh cells, which increases exponentially with every iteration, shown with the green line. The blue line presents the marked mesh cells. The red dotted line shows a threshold of minimum mesh cells that have to be marked for refinement. Therefore, for $min_ref = 0.1$, that number is obtained.

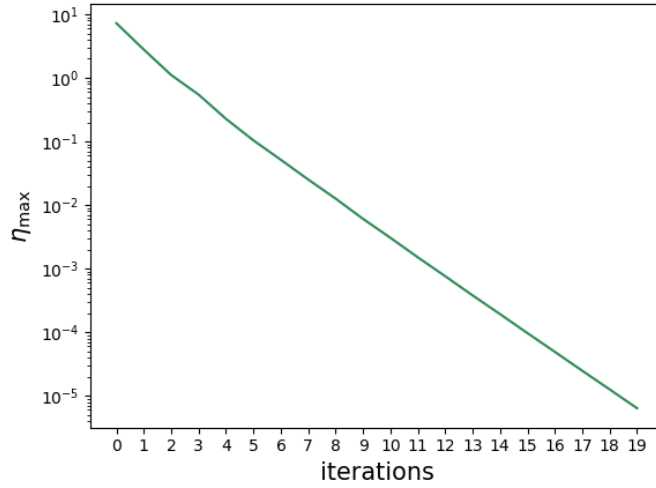


Figure 15: Decreasing values of η_{\max}

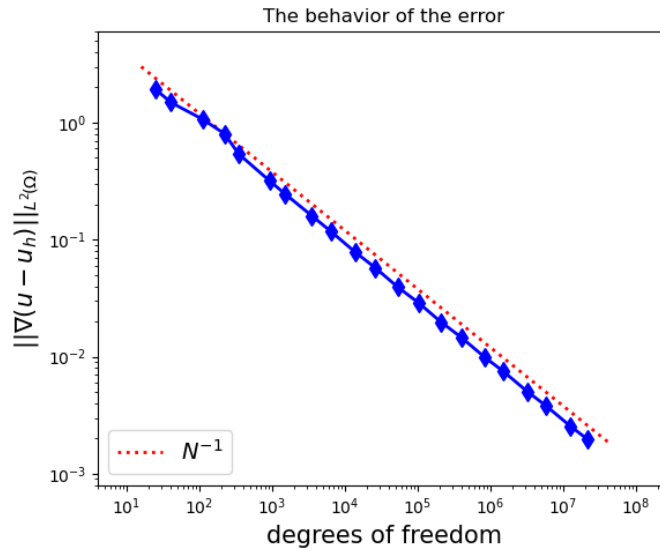


Figure 16: The decrease of the error $\|\nabla(u - u_h)\|_{L^2(\Omega)}$ with respect to the degrees of freedom

As expected, the value of η_{\max} that directs the refinement process, decreases (Figure 15). One can conclude that the value of $\eta_{R,K}$ also decreases.

Figure 16 presents the decreasing values of the error $\|\nabla(u - u_h)\|_{L^2(\Omega)}$ while the values of degrees of freedom increase. The error decreases towards 0. Therefore, as in the previous example, one can conclude that the adaptive Algorithm 3.1 converges. The error decreases optimally following the red dotted line, which presents the optimal decrease of the error. The order of convergence is the first order. The data from 20 iterations is used.

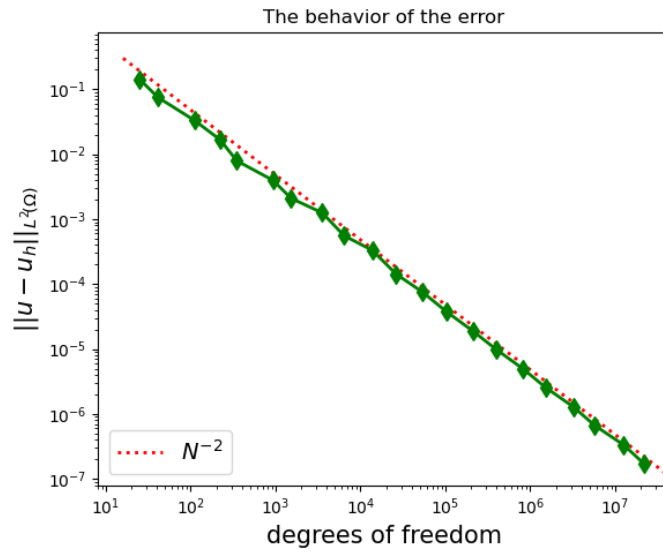


Figure 17: The decrease of the error $\|u - u_h\|_{L^2(\Omega)}$ with respect to the degrees of freedom

In Figure 17, one can see that the error $\|u - u_h\|_{L^2(\Omega)}$ also decreases as the number of degrees of freedom increases. In that case, the second order convergence is obtained.

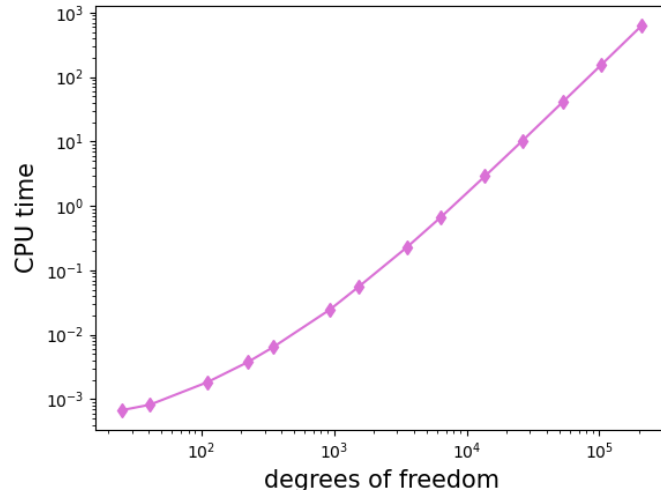


Figure 18: The increase of CPU time

As in the previous example, the computation time increases with increasing the number of degrees of freedom. In Figure 18, one can see results after 13 iterations and significant growth after the number of degrees of freedom exceed 10^3 .

6 Conclusion and Outlook

6.1 Conclusion

This thesis discusses the convergence of the adaptive finite element method for the Poisson problem. It is proved that an adaptive method based on a residual error estimates and a refinement strategy converges to the solution of the Poisson equation. This result is supported by the numerical results of simulations of the Poisson equation for two different examples.

The conforming finite element method is based on the variational form. Variational forms use functions in Sobolev spaces. The Poisson equation with Dirichlet-Neumann boundary conditions is rewritten in its variational form, and then the solution is approximated with the Ritz-Galerkin method in finite element spaces.

It is concluded that a priori error estimates are not sufficient for adaptive methods since they provide only the asymptotic behavior of the discretization errors, while a posteriori error estimates provide reliable upper and lower bounds for the error. The steps for obtaining these bounds are presented as well as an a posteriori error indicator. Having a residual a posteriori error indicator, an adaptive algorithm and refinement strategies are operative. The idea is to refine elements that give a large contribution to the estimated error.

The convergence is proved for cases when the right-hand side is piecewise constant and when the right-hand side is general. It is proved that by every iteration of the adaptive algorithm, the error in the L^2 -norm of gradient is reduced by some fixed factor. Thus the adaptive algorithm converges.

The results from simulations support the theory. It is shown how the values of error in L^2 -norm of gradient decrease while the number of degrees of freedom increases and that the order of convergence is the first order. The examples presented here show the adaptive mesh refinement accurately. They have a boundary layer and an internal layer, which is where singularities appear. Those regions should be refined more, therefore more grid points are placed there. One can see that in the examples, the refinement process is concentrated around the boundary layer and the internal layer, where more grid points are placed.

6.2 Outlook

From the viewpoint of the computations, several additional studies would be possible. The choice of the coarsest grid directs the course of the refinement process. Also, a different level as a starting level for adaptive grid refinement, after the uniform grid refinement, would show a difference. Furthermore, another strategy could be used as a marking strategy to obtain better results. In the examples here the maximum strategy is used as a marking strategy. If maximum marking strategy changes the values of β and *min_ref* the computations would change a lot. Also, to have an efficient adaptive algorithm for the solution of stationary problems, after an adaptive refinement step, a sufficient increase in the number of degrees of freedom is needed. As it is shown, the increasing number of degrees of freedom requires more computation time. Therefore, some balance and optimality between the number of degrees of freedom and computation time should be obtained.

From the mathematical viewpoint, the next step would be to try to use

different a posteriori error estimates to show the convergence of the adaptive algorithm since the refinement strategies work with them. Also, since the convergence is shown in the case with pure Dirichlet boundary conditions, the case with more complicated boundary conditions could be investigated. Eventually, the more complicated partial differential equations could be studied.

List of Figures

1	Red, blue and green refinement [CM10, Figure 6.1.]	26
2	Marked edge bisection [Ver13, Figure 2.5.]	27
3	Uniform and adaptive triangulations [Che05, Figure 6.8.]	29
4	The program flow [Joh00, Figure 1.]	34
5	A known two dimensional solution with a boundary layer	35
6	Development of adaptive meshes through iterations of Algorithm 2.1.	36
7	Decreasing values of η_{\max} through iterations	37
8	The behavior of the error $\ \nabla(u - u_h)\ _{L^2(\Omega)}$ for adaptive refinement	37
9	The behavior of the error $\ u - u_h\ _{L^2(\Omega)}$ with respect to the num- ber of degrees of freedom	38
10	CPU time in seconds through 15 iterations	38
11	Solution of the example 4.2	39
12	Initial grid	39
13	Adaptive refinement of meshes	40
14	Increasing number of mesh cells through iterations	40
15	Decreasing values of η_{\max}	41
16	The decrease of the error $\ \nabla(u - u_h)\ _{L^2(\Omega)}$ with respect to the degrees of freedom	41
17	The decrease of the error $\ u - u_h\ _{L^2(\Omega)}$ with respect to the degrees of freedom	42
18	The increase of CPU time	43

List of Tables

1	Table with information to the number of mesh cells	35
---	--	----

References

- [ABR17] Alejandro Allendes, Gabriel R. Barrenechea, and Richard Rankin. Fully computable error estimation of a nonlinear, positivity-preserving discretization of the convection-diffusion-reaction equation. *SIAM Journal on Scientific Computing*, 39(5):A1903–A1927, 9 2017. Acceptance date: 23/03/17.
- [Ada75] Robert A. Adams. *Sobolev spaces*. Academic Press [A subsidiary of Harcourt Brace Jovanovich, Publishers], New York-London, 1975. Pure and Applied Mathematics, Vol. 65.
- [AF03] Robert A. Adams and John J. F. Fournier. *Sobolev spaces*, volume 140 of *Pure and Applied Mathematics (Amsterdam)*. Elsevier/Academic Press, Amsterdam, second edition, 2003.
- [Beb03] M. Bebendorf. A note on the Poincaré inequality for convex domains. *Z. Anal. Anwendungen*, 22(4):751–756, 2003.
- [BR78] I. Babuška and W. C. Rheinboldt. Error estimates for adaptive finite element computations. *SIAM J. Numer. Anal.*, 15(4):736–754, 1978.
- [BS97] Randolph E. Bank and R. Kent Smith. Mesh smoothing using a posteriori error estimates. *SIAM J. Numer. Anal.*, 34(3):979–997, 1997.
- [BS08] Susanne C. Brenner and L. Ridgway Scott. *The mathematical theory of finite element methods*, volume 15 of *Texts in Applied Mathematics*. Springer, New York, third edition, 2008.
- [Che05] Zhangxin Chen. *Finite element methods and their applications*. Scientific Computation. Springer-Verlag, Berlin, 2005.
- [Cia91] P. G. Ciarlet. Basic error estimates for elliptic problems. In *Handbook of numerical analysis, Vol. II*, Handb. Numer. Anal., II, pages 17–351. North-Holland, Amsterdam, 1991.
- [CM10] C. Carstensen and C. Merdon. Estimator competition for Poisson problems. *J. Comput. Math.*, 28(3):309–330, 2010.
- [Cou43] R. Courant. Variational methods for the solution of problems of equilibrium and vibrations. *Bull. Amer. Math. Soc.*, 49:1–23, 1943.
- [Dör96] Willy Dörfler. A convergent adaptive algorithm for Poisson’s equation. *SIAM J. Numer. Anal.*, 33(3):1106–1124, 1996.
- [DD12] Françoise Demengel and Gilbert Demengel. *Functional spaces for the theory of elliptic partial differential equations*. Universitext. Springer, London; EDP Sciences, Les Ulis, 2012. Translated from the 2007 French original by Reinie Erné.
- [EG04] Alexandre Ern and Jean-Luc Guermond. *Theory and practice of finite elements*, volume 159 of *Applied Mathematical Sciences*. Springer-Verlag, New York, 2004.

- [ESW05] Howard C. Elman, David J. Silvester, and Andrew J. Wathen. *Finite elements and fast iterative solvers: with applications in incompressible fluid dynamics*. Numerical Mathematics and Scientific Computation. Oxford University Press, New York, 2005.
- [Far16] Douglas Farenick. *Fundamentals of functional analysis*. Universitext. Springer, Cham, 2016.
- [GB05] Thomas Grätsch and Klaus-Jürgen Bathe. A posteriori error estimation techniques in practical finite element analysis. *Comput. & Structures*, 83(4-5):235–265, 2005.
- [Gri11] Pierre Grisvard. *Elliptic problems in nonsmooth domains*, volume 69 of *Classics in Applied Mathematics*. Society for Industrial and Applied Mathematics (SIAM), Philadelphia, PA, 2011. Reprint of the 1985 original [MR0775683], With a foreword by Susanne C. Brenner.
- [Han05] Weimin Han. *A posteriori error analysis via duality theory*, volume 8 of *Advances in Mechanics and Mathematics*. Springer-Verlag, New York, 2005. With applications in modeling and numerical approximations.
- [JM04] Volker John and Gunar Matthies. MooNMD—a program package based on mapped finite element methods. *Comput. Vis. Sci.*, 6(2-3):163–169, 2004.
- [JMT97] V. John, J. M. Maubach, and L. Tobiska. Nonconforming streamline-diffusion-finite-element-methods for convection-diffusion problems. *Numer. Math.*, 78(2):165–188, 1997.
- [Joh00] Volker John. A numerical study of a posteriori error estimators for convection-diffusion equations. *Comput. Methods Appl. Mech. Engrg.*, 190(5-7):757–781, 2000.
- [JS08] Volker John and Ellen Schmeyer. Finite element methods for time-dependent convection-diffusion-reaction equations with small diffusion. *Comput. Methods Appl. Mech. Engrg.*, 198(3-4):475–494, 2008.
- [LB13] Mats G. Larson and Fredrik Bengzon. *The finite element method: theory, implementation, and applications*, volume 10 of *Texts in Computational Science and Engineering*. Springer, Heidelberg, 2013.
- [Maz85] Vladimir G. Maz’ja. *Sobolev spaces*. Springer Series in Soviet Mathematics. Springer-Verlag, Berlin, 1985. Translated from the Russian by T. O. Shaposhnikova.
- [MNS02] Pedro Morin, Ricardo H. Nochetto, and Kunibert G. Siebert. Convergence of adaptive finite element methods. *SIAM Rev.*, 44(4):631–658 (2003), 2002. Revised reprint of “Data oscillation and convergence of adaptive FEM” [SIAM J. Numer. Anal. **38** (2000), no. 2, 466–488 (electronic); MR1770058 (2001g:65157)].

- [OR76] J. T. Oden and J. N. Reddy. *An introduction to the mathematical theory of finite elements*. Wiley-Interscience [John Wiley & Sons], New York-London-Sydney, 1976. Pure and Applied Mathematics.
- [SF73] Gilbert Strang and George J. Fix. *An analysis of the finite element method*. Prentice-Hall, Inc., Englewood Cliffs, N. J., 1973. Prentice-Hall Series in Automatic Computation.
- [SS05] Alfred Schmidt and Kunibert G. Siebert. *Design of adaptive finite element software*, volume 42 of *Lecture Notes in Computational Science and Engineering*. Springer-Verlag, Berlin, 2005. The finite element toolbox ALBERTA, With 1 CD-ROM (Unix/Linux).
- [Ver94] R. Verfürth. A posteriori error estimation and adaptive mesh-refinement techniques. In *Proceedings of the Fifth International Congress on Computational and Applied Mathematics (Leuven, 1992)*, volume 50, pages 67–83, 1994.
- [Ver13] Rüdiger Verfürth. *A posteriori error estimation techniques for finite element methods*. Numerical Mathematics and Scientific Computation. Oxford University Press, Oxford, 2013.
- [WBA⁺17] Ulrich Wilbrandt, Clemens Bartsch, Naveed Ahmed, Najib Alia, Felix Anker, Laura Blank, Alfonso Caiazzo, Sashikumaar Ganesan, Svetlana Giere, Gunar Matthies, Raviteja Meesala, Abdus Shamim, Jagannath Venkatesan, and Volker John. ParMooN—A modernized program package based on mapped finite elements. *Comput. Math. Appl.*, 74(1):74–88, 2017.

A Tools from the Analysis

This chapter consists of the necessary mathematical results, definitions, and notations from functional analysis needed for this thesis.

Notation. The notation Γ stands for the boundary of Ω . The notation $\overline{\Omega}$ stands for the closure of the Ω .

Let $\alpha = (\alpha_1, \alpha_2, \dots, \alpha_n)$ be called a multi-index defined as an n -tuple of nonnegative integers α_j . Let x^α denote the monomial $x_1^{\alpha_1} \cdots x_n^{\alpha_n}$, which has degree $|\alpha| = \sum_{j=1}^n \alpha_j$. If $D_j = \frac{\partial}{\partial x_j}$ then $D^\alpha = D_1^{\alpha_1} \cdots D_n^{\alpha_n}$ denotes a differential operator of order $|\alpha|$. Note that $D^{(0, \dots, 0)}u$ is equal to u .

Laplacian operator Δ is defined as

$$\Delta p = \frac{\partial^2 p}{\partial x_1^2} + \frac{\partial^2 p}{\partial x_2^2}.$$

Definition 1. (*Essentially bounded*) Let (X, Σ, μ) be a measurable space. The essential supremum of a measurable function $u : X \rightarrow \mathbb{C}$ is the quantity

$$\text{ess sup } u = \sup \left\{ |\lambda| : \lambda \in \bigcap_{E \in \Sigma, \mu(E^c)=0} \overline{u(E)} \right\}.$$

If the essential supremum of u is finite, then u is essentially bounded. This definition can be found in [Far16, Def. 5.46].

Definition 2. (*Banach space*) A normed linear space $(V, \|\cdot\|)$ is called a Banach space if it is complete with respect to the metric induced by the norm $\|\cdot\|$. This definition can be found in [BS08, Def. 1.1.7].

Definition 3. (*Space $C^m(\Omega)$*) Let m be any nonnegative integer and let $C^m(\Omega)$ denote the vector space consisting of all functions u which, together with all their partial derivatives $D^\alpha u$ of orders $|\alpha| \leq m$, are continuous on Ω . This definition is taken from [AF03, Def. 1.26].

Definition 4. (*Space $C^\infty(\Omega)$*) The space $C^\infty(\Omega)$ is the space of infinitely differentiable functions on Ω , as defined in [Maz85, Page 1.].

Definition 5. (*Space of bounded, continuous functions*) The space $C_B^m(\Omega)$ consists of all functions $u \in C^m(\Omega)$ for which $D^\alpha u$ is bounded on Ω for $0 \leq |\alpha| \leq m$. It is a Banach space with the norm:

$$\|u\|_{C_B^m(\Omega)} = \max_{0 \leq |\alpha| \leq m} \sup_{x \in \Omega} |D^\alpha u(x)|.$$

The definition can be found in [AF03, Def. 1.27].

Definition 6. (*Space of bounded, uniformly continuous functions*)

If $u \in C(\Omega)$ is bounded and uniformly continuous on Ω , then it possesses a unique, bounded, continuous extension to the $\overline{\Omega}$. The vector space $C^m(\overline{\Omega})$

consists of all functions $u \in C^m(\Omega)$ for which $D^\alpha u$ is bounded and uniformly continuous on Ω for $0 \leq |\alpha| \leq m$. It has the norm:

$$\|u\|_{C^m(\bar{\Omega})} = \max_{0 \leq |\alpha| \leq m} \sup_{x \in \Omega} |D^\alpha u(x)|.$$

$C^m(\bar{\Omega})$ is a closed subspace of $C_B^m(\Omega)$, thus it is a Banach space. This definition can be found in [AF03, Def. 1.28].

Definition 7. (*Space of Hölder continuous functions*) Let $0 < \lambda \leq 1$ and let $C^{m,\lambda}(\bar{\Omega})$ denote the space consisting of functions u for which $D^\alpha u$, whenever $0 \leq |\alpha| \leq m$, satisfies a Hölder condition of exponent λ in Ω . That means that there exists a constant C such that

$$|D^\alpha u(x) - D^\alpha u(y)| \leq C|x - y|^\lambda, \quad x, y \in \Omega.$$

The space $C^{m,\lambda}(\bar{\Omega})$ is a subspace of $C^m(\bar{\Omega})$, thus it is a Banach space with the norm:

$$\|u\|_{C^{m,\lambda}(\bar{\Omega})} = \|u\|_{C^m(\bar{\Omega})} + \max_{0 \leq |\alpha| \leq m} \sup_{x,y \in \Omega, x \neq y} \frac{|D^\alpha u(x) - D^\alpha u(y)|}{|x - y|^\lambda}.$$

The definition can be found in [AF03, Def. 1.29].

Definition 8. (*Hilbert space*) Let X be a vector space and $(\cdot, \cdot)_X$ a functional defined on $X \times X$. A functional $(\cdot, \cdot)_X$ is called an inner product on X if for every $x, y \in X$ and $a, b \in \mathbb{C}$ it holds:

- i) $(x, y)_X = \overline{(y, x)_X}$,
- ii) $(ax + by, z)_X = a(x, z)_X + b(y, z)_X$,
- iii) $(x, x)_X = 0$ if and only if $x = 0$.

A space X is called an inner product space if it is equipped with an inner product. A norm on X is defined as $\|x\|_X = \sqrt{(x, x)_X}$. If X is a Banach space under this norm, then X is called a Hilbert space. This definition is taken from [AF03, Def. 1.10].

Definition 9. (*Dual space*) The dual space denoted by B' is a set of bounded linear functionals on a Banach space B as defined in [Che05, Page 25].

Definition 10. (*Support of a function*) If u is a function defined on Ω , then the support of u is defined as the set

$$\text{supp}(u) = \overline{\{x \in \Omega : u(x) \neq 0\}}.$$

The definition is taken from [AF03, Def. 1.3].

Definition 11. (*Lipschitz domain, Lipschitz boundary*) An open subset $\Omega \subset \mathbb{R}^n$ is called Lipschitz domain and Γ is called Lipschitz boundary if for every $x \in \Gamma$ there exists a neighbourhood U of x in \mathbb{R}^n and new orthogonal coordinates $\{y_1, \dots, y_n\}$ such that

a) U is an hypercube in the new coordinates:

$$U = \{(y_1, \dots, y_n) \mid -a_i < y_i < a_i, 1 \leq i \leq n\}$$

b) there exists a Lipschitz continuous function φ , defined in

$$U' = \{(y_1, \dots, y_{n-1}) \mid -a_i < y_i < a_i, 1 \leq i \leq n-1\},$$

such that

$$\begin{aligned} |\varphi(y')| &\leq \frac{a_n}{2} \text{ for every } y' = (y_1, \dots, y_{n-1}) \in U', \\ \Omega \cap U &= \{y = (y', y_n) \in U \mid y_n < \varphi(y')\}, \\ \Gamma \cap U &= \{y = (y', y_n) \in U \mid y_n = \varphi(y')\}. \end{aligned}$$

The definition can be found in [Gri11, Def. 1.2.1.1]. Only domains with Lipschitz boundary are considered in this thesis.

The following definitions can be found in [Che05, Page 26-27].

Definition 12. (*Bilinear form*) Let V be a Hilbert space with the scalar product (\cdot, \cdot) and the corresponding norm $\|\cdot\|_V$, then $a(\cdot, \cdot) : V \times V \rightarrow \mathbb{R}$ is a bilinear form, if it satisfies:

$$\begin{aligned} i) \quad &a(u, \alpha v + \beta w) = \alpha a(u, v) + \beta a(u, w), \\ ii) \quad &a(\alpha u + \beta v, w) = \alpha a(u, w) + \beta a(v, w), \end{aligned}$$

for $\alpha, \beta \in \mathbb{R}$, and $u, v, w \in V$.

Definition 13. A bilinear form $a(\cdot, \cdot)$ is symmetric for all $u, v \in V$, if

$$a(u, v) = a(v, u).$$

Definition 14. A bilinear form $a(\cdot, \cdot)$ is called continuous or bounded in the norm $\|\cdot\|_V$, if there exists a constant $M > 0$ such that

$$|a(u, v)| \leq M \|u\|_V \|v\|_V$$

for every $u, v \in V$.

Definition 15. A bilinear form $a(\cdot, \cdot)$ is called coercive or V -elliptic, if there exists a constant $m > 0$ such that

$$|a(u, u)| \geq m \|u\|_V^2$$

for every $u \in V$.

Definition 16. (*Green's formula*) Let Ω be a domain in \mathbb{R}^2 , Γ boundary and n an exterior unit normal. Green's formula is defined as

$$\int_{\Omega} -\Delta u \cdot v dx = \int_{\Omega} \nabla u \cdot \nabla v dx - \int_{\Gamma} n \cdot \nabla u v ds.$$

Green's formula also holds in higher dimensional spaces. This definition can be found in [LB13, Def. 4.4].

Definition 17. (*Dirichlet boundary condition*) The Dirichlet boundary condition provides the value of the solution at the boundary, as defined in [LB13, 2.2.2.1]. Also, it is called an essential condition, because it appears explicitly in the variational formulation i.e., in the definition of the space V [BS08, Page 3].

Definition 18. (*Neumann boundary condition*) The Neumann boundary condition provides the value of the solution derivative at the boundary, as defined in [LB13, 2.2.2.1]. Also, it is called a natural condition, because it is incorporated implicitly. It is denoted by $\frac{\partial u}{\partial n}$, i.e. a derivative of u in the direction normal to the boundary Γ . It can be equivalently written as $\frac{\partial u}{\partial n} = n \cdot \nabla u$ [BS08, Page 3, Page 129].

Theorem A.1. (*Riesz Representation Theorem*) Let V be a Hilbert space with inner product (\cdot, \cdot) . Every continuous linear form $f(\cdot)$ on V can be uniquely represented as

$$f(v) = (u, v)$$

for some $u \in V$.

Proof. The proof can be found in [LB13], Theorem 7.1. \square

Theorem A.2. Let V be a Hilbert space, and let $a(\cdot, \cdot)$ be a continuous, symmetric, coercive bilinear form on V . Then the variational problem is equivalent to the minimization problem: find $u \in V$ such that $F(u) = \min_{v \in V} F(v)$ where $F(v) = \frac{1}{2}a(v, v) - f(v)$.

Proof. This proof can be found in [LB13], Theorem 7.2. \square

Definition 19. (*Diameter h_K*) A diameter h_K of an arbitrary element $K \in \mathcal{T}^h$ is defined as

$$h_K = \text{diam}(K) = \max\{|x - y| : x, y \in K\}.$$

For a triangulation T^h , we denote $h = \max_{K \in T^h} h_K$ a mesh parameter. It is a measure of how refined the mesh is. The smaller h is, the finer the mesh. This definition can be found in [Han05, Page 40]. A diameter of every element or edge $F \in \mathcal{T}^h \cup \mathcal{E}$ is denoted by h_F [Ver13, Page 5].

Lemma A.1. (*Deny-Lions*) Let $1 \leq p \leq +\infty$ and $l \geq 0$. Let Ω be a connected bounded open set having the $(1, p)$ -extension property. There exists $c > 0$ such that

$$\forall v \in W^{l+1,p}(\Omega), \quad \inf_{\pi \in P_l} \sum_{|\alpha| \leq l+1} \|D^\alpha(v + \pi)\|_{L^p(\Omega)} \leq c \sum_{|\alpha|=l+1} \|D^\alpha v\|_{L^p(\Omega)}.$$

Proof. This proof can be found in [EG04], Lemma B.67. \square

Lemma A.2. (*Bramble-Hilbert*) Assume the hypotheses of the Deny-Lions Lemma hold. Then, there is $c > 0$ such that, for all $f \in (W^{k+1,p}(\Omega))'$ vanishing on P_k ,

$$\forall v \in W^{k+1,p}(\Omega), \quad |f(v)| \leq c \|f\|_{(W^{k+1,p}(\Omega))'} \sum_{|\alpha|=k+1} \|D^\alpha v\|_{L^p(\Omega)}.$$

Proof. This proof can be found in [EG04], Lemma B.68. \square

Definition 20. (*Fractional Sobolev spaces*) For $0 < s < 1$ and $1 \leq p < +\infty$, the Sobolev space with fractional exponent is defined as

$$W^{s,p}(\Omega) = \left\{ u \in L^p(\Omega) : \frac{u(x) - u(y)}{\|x - y\|^{s+\frac{d}{p}}} \in L^p(\Omega \times \Omega) \right\}.$$

This definition can be found in [EG04, Def. B.30]. Using mappings, it is possible to define $W^{s,p}(\partial\Omega)$ whenever $\partial\Omega$ is a smooth manifold.

Theorem A.3. (*Trace Theorem 1*) *Let $1 \leq p < +\infty$ and Ω be a Lipschitz bounded open set. Then,*

- (i) $\gamma_0 : W^{1,p}(\Omega) \rightarrow W^{\frac{1}{p'},p}(\partial\Omega)$ *is surjective.*
- (ii) *The kernel of γ_0 is $W_0^{1,p}(\Omega)$.*

Proof. More details in [EG04], Theorem B.52. □

Corollary A.1. *Let $1 \leq p < +\infty$ and Ω be a Lipschitz bounded open set. Then, there exists a constant c such that, for all $g \in W^{\frac{1}{p'},p}(\partial\Omega)$, there exists $u_g \in W^{1,p}(\Omega)$ satisfying $\gamma_0(u_g) = g$ and $\|u_g\|_{W^{1,p}(\Omega)} \leq c\|g\|_{W^{\frac{1}{p'},p}(\partial\Omega)}$. The function u_g is said to be a lifting of g in $W^{1,p}(\Omega)$.*

Proof. More details in [EG04], Corollary B.53. □

Theorem A.4. *Let $\Omega \subset \mathbb{R}^n$ be a convex domain with diameter d . Then*

$$\|u\|_{L^2(\Omega)} \leq \frac{d}{\pi} \|\nabla u\|_{L^2(\Omega)}$$

for all $u \in H^1(\Omega)$ satisfying $\int_{\Omega} u(x)dx = 0$.

Proof. This proof can be found in [Beb03], Theorem 3.2. □

Nomenclature

(\cdot, \cdot)	inner product of $L^2(\Omega)$, page 3
$(\cdot, \cdot)_{H^m(\Omega)}$	inner product of $H^m(\Omega)$, page 7
\mathbf{n}_e	unit normal vector to edge e , page 21
\mathbf{n}_K	unit outward normal to the element K , page 22
Δ	Laplacian operator, page 8
δ_{ij}	Kronecker delta, page 11
η_{\max}	maximum value of $\eta_{R,K}$, $K \in \mathcal{T}^h$, page 24
$\eta_{R,K}$	residual a posteriori error indicator, page 23
Γ	boundary, page 4
γ	trace map, page 7
Γ_D	Dirichlet boundary, page 8
Γ_N	Neumann boundary, page 8
\hat{K}	reference triangle or reference square, page 11
$\hat{P}(\hat{K})$	polynomial space, page 14
Λ	all edges in \mathcal{E} , page 21
λ_n	nodal shape function of a vertex n , page 22
$\ \cdot\ _{C^j(\bar{\Omega})}$	norm of $C^j(\bar{\Omega})$, page 5
$\ \cdot\ _{H^m(\Omega)}$	norm of $H^m(\Omega)$, page 7
$\ \cdot\ _{L^p}$	norm of $L^p(\Omega)$, page 3
$\ \cdot\ _{L^\infty}$	norm of $L^\infty(\Omega)$, page 3
$\ \cdot\ _{W^{m,\infty}(\Omega)}$	norm of $W^{m,\infty}(\Omega)$, page 4
$\ \cdot\ _{W^{m,p}(\Omega)}$	norm of $W^{m,p}(\Omega)$, page 4
$\mathcal{J}_e(\cdot)$	jump across edge e , page 21
\mathcal{N}	set of all vertices associated with \mathcal{T}^h , page 22
\mathcal{N}_{Γ_N}	vertices on Γ_N , page 22
\mathcal{N}_Ω	interior vertices, page 22
$\mathcal{R}(v)$	residual of $u_{\mathcal{T}^h}$, page 21
\mathcal{T}^h	mesh, page 10
\mathcal{E}	edges corresponding to \mathcal{T}^h , page 21

\mathcal{E}_Γ	edges on Γ , page 21
\mathcal{E}_{Γ_D}	edges on Γ_D , page 21
\mathcal{E}_{Γ_N}	edges on Γ_N , page 21
\mathcal{E}_Ω	interior edges, page 21
∇	nabla or gradient operator, page 7
Ω	domain, page 3
$\Phi_n(\cdot)$	linear functionals, page 11
ψ_K	mapping from $V(K)$ to $V(\hat{K})$, page 14
ρ_K	diameter of the largest ball inscribed in K , page 14
$\sigma_{\mathcal{T}^h}$	shape parameter of \mathcal{T}^h , page 22
θ_n	shape functions, page 11
\tilde{g}	lifting of g , page 16
φ	Lipschitz function, page 17
$\tilde{\mathcal{T}}^h$	subset of marked elements for mesh refinement, page 25
\tilde{K}_e	union of all elements sharing a vertex with e , page 22
\tilde{K}_n	union of all elements that share a vertex with K , page 22
A	stiffness matrix, page 10
$a(\cdot, \cdot)$	bilinear form, page 50
b	load vector, page 10
B_K	Jacobian matrix, page 14
$C^j(\bar{\Omega})$	space of bounded, uniformly continuous functions, page 48
$C_B^j(\Omega)$	space of bounded continuous functions, page 48
$C^\infty(\Omega)$	space of infinitely differentiable functions, page 48
$C_0^\infty(\Omega)$	function space, page 4
$C^{j,\lambda}(\bar{\Omega})$	space of Hölder continuous functions, page 49
D^α	derivative, page 4
E	(m, p) -extension operator, page 5
F_K	affine diffeomorphism, page 11
f_K	mean value of function f , page 23
$f_{\mathcal{T}^h}$	L^2 -projection of f onto the space of piecewise constant functions corresponding to \mathcal{T}^h , page 30

g_e mean value of function g , page 23
 h maximum value of h_K , $K \in \mathcal{T}^h$, page 51
 $H_0^1(\Omega)$ Sobolev space, page 7
 $H_D^1(\Omega)$ Sobolev space, page 8
 $H_{g_D, D}^1(\Omega)$ Sobolev space, page 18
 $H^m(\Omega)$ Sobolev space, page 7
 $H^{\frac{1}{2}}(\Gamma)$ trace of a function in $H^1(\Omega)$, page 16
 h_e diameter of e , page 51
 h_K diameter of K , page 51
 I_h global interpolation operator, page 14
 I_h^1 Lagrangian piecewise linear interpolation operator, page 12
 I_K local interpolation operator, page 14
 $I_{\hat{K}}$ local interpolation operator, page 14
 $I_{\mathcal{T}^h}$ interpolation operator that maps $H_D^1(\Omega)$ to $S_D^{1,0}(\mathcal{T}^h)$, page 22
 j edge residuals, page 22
 K_e a union of all elements sharing an edge with K , page 23
 K_n union of all elements having n as a vertex, page 22
 $L^p(\Omega)$ Lebesgue space, page 3
 $L^\infty(\Omega)$ Lebesgue space, page 3
 $L_{loc}^1(\Omega)$ space of locally integrable functions, page 4
 n outward unit normal vector, page 8
 n_x inward normal to Γ at x , page 5
 P_K space spanned by restrictions of v_h to K , page 11
 P_m m -th order approximation space, page 16
 q quality function, page 27
 r element residuals, page 22
 $R_1(K)$ first order polynomials on element K , page 11
 $S^{1,0}(\mathcal{T}^h)$ lowest order conforming finite element space corresponding to \mathcal{T}^h , page 11
 $S_D^{1,0}(\mathcal{T}^h)$ lowest order conforming finite element space corresponding to \mathcal{T}^h vanishing on Γ_D , page 11

U_x neighborhood of $x \in \Gamma$, page 5
 $V(\hat{K})$ domain of the interpolation operator, page 14
 $W^{m,p}(\Omega)$ Sobolev space, page 4
 $W_0^{m,p}(\Omega)$ Sobolev space, page 6
 w_K integral mean value of w over K , page 31
 w_{K_n} is the average of w on K_n , page 22